AD-A163 706 THE CLASSIFICATION OF SOLUTIONS OF QUADRATIC RIEMANN PROBLEMS (I)(U) WISCONSIN UNIV-MADISON MATHEMATICS RESEARCH CENTER E ISAACSON ET AL. DEC 85 MRC-TSR-2891 1/1

UNCLASSIFIED DAAG29-80-C-0041 F/G 12/1 NL

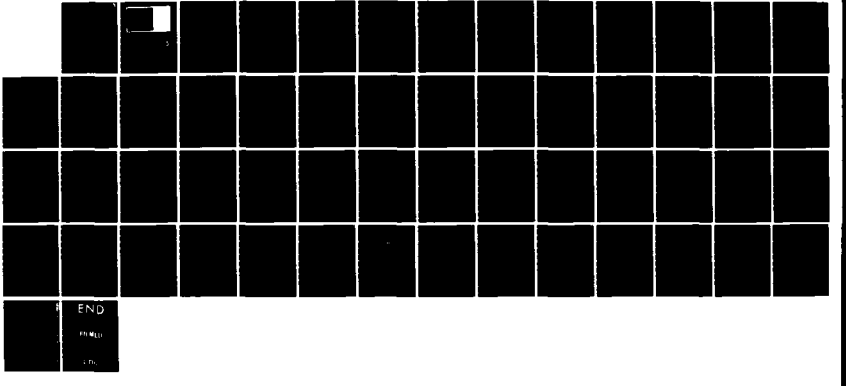

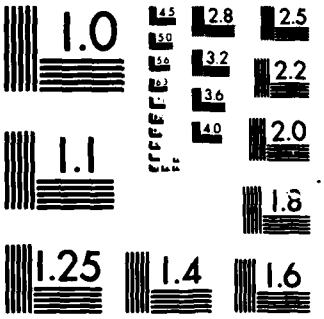

MRC Technical Summary Report #2891

THE CLASSIFICATION OF SOLUTIONS OF QUADRATIC RIEMANN PROBLEMS (I)

E. Isaacson, D. Marchesin,
B. Plohr and B. Temple

Mathematics Research Center
University of Wisconsin—Madison
610 Walnut Street
Madison, Wisconsin 53705

December 1985

(Received August 8, 1985)

Sponsored by

U. S. Army Research Office
P. O. Box 12211
Research Triangle Park
North Carolina 27709

National Science Foundation
Washington, DC 20550

UNIVERSITY OF WISCONSIN-MADISON
MATHEMATICS RESEARCH CENTER

THE CLASSIFICATION OF SOLUTIONS OF QUADRATIC RIEMANN PROBLEMS (I)*

E. Isaacson**[4,5,9,10,11], D. Marchesin***[3,4,5], B. Plohr[4,5,7,8] and B. Temple[1,2,6,7,8]

Technical Summary Report #2891
December 1985

ABSTRACT

We are interested in classifying the solutions of Riemann problems for the 2×2 conservation laws which have homogeneous quadratic flux functions. Such flux functions approximate an arbitrary 2×2 system in a neighborhood of an isolated point where strict hyperbolicity fails. This problem was motivated by Marchesin and Paes-Leme who discovered such a singularity in a system of equations arising in oil reservoir simulation, [15,17]. In [18], Schaeffer, Shearer, Marchesin and Paes-Leme solved the Riemann problem for this system in a neighborhood of the singular point. In [8], Isaacson and Temple outlined a program for classifying such singularities by means of locating normal forms for the equivalence classes of equations generated by linear changes in dependent variables. A 2-parameter family of such normal forms was found by Plohr. In the important work of Schaeffer and Shearer [17], a new normal form was found which reduced the classification of integral curves to a theorem of Darboux on the classification of umbilic

*Appeared as PUC/RJ Report MAT 12-85.

**Department of Mathematics, University of Wyoming, Laramie, Wyoming.
***Department of Mathematics, PUC/RJ, 22453 Rio de Janeiro, Brazil.

[1]Supported in part by FINEP/Brazil Grant No. 4.3.82.017.9.
[2]Supported in part by CNPq/Brazil Grant No. 1.01.10.011/84-ACI.
[3]Supported in part by CNPq/Brazil Fellowship No. 30.0204/83-MA.
[4]Supported in part by NSF Grant No. DMS-831229.
[5]Supported in part by DOE Contract No. DE-AC02-76ER03077.
[6]Supported in part by NSF Grant No. 5274298INT-8415209.
[7]Sponsored by the United States Army under Contract No. DAAG29-80-C-0041.
[8]This material is based upon work supported by the National Science Foundation under Grant No. DMS-8210950, Mod. 1.
[9]Supported in part by University of Wyoming Division of Basic Research.
[10]Supported in part by AFOSR Grant No. AFOSR-85-0117.
[11]Supported in part by CNPq/Brazil Grant No. 403039/84-MA.

points for homogeneous cubic equations [3]. The integral curves fall into four isomorphism classes, called Regions I-IV. In this paper we give the solution of the Riemann problem for the systems in Region IV which exhibit up-down symmetry. A presentation of the solutions of the corresponding systems in Regions II and III will follow.

Our analysis uses a numerical determination of the Hugoniot loci. Moreover, a new phenomenon occurs in Regions II-IV that does not occur in Region I: lines exist on which one of the eigenvalues has the value of the eigenvalue at the singular point. Bifurcations occur at these lines, and the dynamics of the lines as the parameters in the normal form are varied gives a geometric interpretation of the boundaries between Regions I-III. The program for classifying hyperbolic singular points in 2×2 systems of conservation laws is being carried out jointly by the authors named above.

AMS (MOS) Subject Classifications: 65M10, 76N99, 35L65, 35L67

Key Words: Riemann problem, non-strictly hyperbolic conservation laws, umbilic points

Work Unit Numbers 1 (Applied Analysis) and 3 (Numerical Analysis and Scientific Computing)

SIGNIFICANCE AND EXPLANATION

A 2×2 system of conservation laws is a system of partial differential equations of the form

$$\underset{\sim}{u}_t + \underset{\sim}{f}(\underset{\sim}{u})_x = 0 \tag{1}$$

where $\underset{\sim}{u} = (u,v)$, $\underset{\sim}{f} = (f,g)$ are in $R \times R$ and where $x \in R$, $t > 0$. Such equations arise in gas dynamics, elasticity, oil reservoir simulation and other areas of engineering when diffusion is neglected. In solutions of (1), information travels at speeds λ_1 and λ_2 given by the eigenvalues of the matrix $\frac{\partial \underset{\sim}{f}}{\partial \underset{\sim}{u}}$. Since this matrix depends on u, v, the speeds λ_1 and λ_2 depend on the solution, and this leads to the formation of discontinuities called shock waves. The present paper deals with the classification of Riemann problem solutions (solutions which evolve from a single discontinuity at time $t = 0$) near an isolated point at which $\frac{\partial \underset{\sim}{f}}{\partial \underset{\sim}{u}}$ is a multiple of the identity, so that $\lambda_1 = \lambda_2$. Such a singularity has no analogue in the linear theory.

THE CLASSIFICATION OF SOLUTIONS OF QUADRATIC RIEMANN PROBLEMS (I)*

E. Isaacson**[4,5,9,10,11], D. Marchesin***[3,4,5], B. Plohr[4,5,7,8] and B. Temple[1,2,6,7,8]

§1. Introduction

We consider the general 2×2 system of conservation laws with quadratic flux functions

$$\begin{aligned} u_t + \frac{1}{2}\{a_1 u^2 + 2b_1 uv + c_1 v^2\}_x &= 0 , \\ v_t + \frac{1}{2}\{a_2 u^2 + 2b_2 uv + c_2 v^2\}_x &= 0 . \end{aligned} \tag{1}$$

In particular, we solve the Riemann problem globally for a specific range of the coefficients a_i, b_i, c_i.

System (1) is of interest because solutions of (1) approximate solutions of an arbitrary 2×2 system of conservation laws

$$\underset{\sim}{u}_t + \underset{\sim}{f}(\underset{\sim}{u})_x = \underset{\sim}{0} , \tag{2}$$

where $\underset{\sim}{u} = (u,v)$, $\underset{\sim}{f} = (f,g)$, in a neighborhood of an isolated hyperbolic singularity. Such a singularity is an isolated point in a neighborhood of which (2) is hyperbolic and at which the Jacobian

$$A(\underset{\sim}{u}) \equiv \frac{\partial \underset{\sim}{f}}{\partial \underset{\sim}{u}} = \begin{bmatrix} f_u & f_v \\ g_u & g_v \end{bmatrix}$$

---

*Appeared as PUC/RJ Report MAT 12-85.

**Department of Mathematics, University of Wyoming, Laramie, Wyoming.
***Department of Mathematics, PUC/RJ, 22453 Rio de Janeiro, Brazil.

---

[1]Supported in part by FINEP/Brazil Grant No. 4.3.82.017.9.
[2]Supported in part by CNPq/Brazil Grant No. 1.01.10.011/84-ACI.
[3]Supported in part by CNPq/Brazil Fellowship No. 30.0204/83-MA.
[4]Supported in part by NSF Grant No. DMS-831229.
[5]Supported in part by DOE Contract No. DE-AC02-76ER03077.
[6]Supported in part by NSF Grant No. 5274298INT-8415209.
[7]Sponsored by the United States Army under Contract No. DAAG29-80-C-0041.
[8]This material is based upon work supported by the National Science Foundation under Grant No. DMS-8210950, Mod. 1.
[9]Supported in part by University of Wyoming Division of Basic Research.
[10]Supported in part by AFOSR Grant No. AFOSR-85-0117.
[11]Supported in part by CNPq/Brazil Grant No. 403039/84-MA.

has equal eigenvalues and is diagonalizable. In fact, system (1) is obtained from system (2) as follows. Let $\lambda_1(\underset{\sim}{u}) \leq \lambda_2(\underset{\sim}{u})$ denote the eigenvalues of $A(\underset{\sim}{u})$, and let $\underset{\sim}{u}_0$ denote the isolated point at which $\lambda_1(\underset{\sim}{u}_0) = \lambda_2(\underset{\sim}{u}_0) \equiv \lambda_0$. First, replace $\underset{\sim}{u}$ by $\underset{\sim}{u} - \underset{\sim}{u}_0$ and translate the reference frame (x,t) to $(x - \lambda_0 t, t)$ so that the resulting system has an isolated singularity at $\underset{\sim}{u} = (0,0)$ with corresponding double eigenvalue $\lambda = 0$. Then system (1) is obtained by expanding the flux functions of this transformed system in Taylor series about $(0,0)$ and neglecting higher order terms.

System (1) can be reduced further by a nonsingular linear change of dependent variables. Two systems related by such a transformation S are isomorphic in the sense that $S\underset{\sim}{u}(x,t)$ is a weak solution of the transformed system if and only if $\underset{\sim}{u}(x,t)$ is a weak solution of the original system. Since the nonsingular transformation S contains four free parameters and since system (1) contains six parameters, we expect to find a two parameter family of isomorphism classes for system (1). Thus, we look for representatives of the isomorphism classes in a normal form containing two free parameters [8]. In what we consider to be a breakthrough, Shearer and Schaeffer showed in [17] that when system (1) is *hyperbolic*, there is a *nonsingular* linear change of dependent variables which transforms system (1) into

$$
\begin{aligned}
u_t + \frac{1}{2}\{au^2 + 2buv + v^2\}_x &= 0 \ , \\
v_t + \frac{1}{2}\{bu^2 + 2uv\}_x &= 0 \ .
\end{aligned}
\tag{3}
$$

System (3) depends on two free parameters a and b and can be taken as a normal form for the hyperbolic quadratic systems (1). It is also shown in [3,17] that the integral curves of (3) fall into four nonisomorphic classes depending on the parameters a and b. These classes define four regions in the a,b-plane which are referred to as Regions I-IV.

The regions are determined by the number of lines which form the Hugoniot locus of the origin, as well as the direction of increase of the appropriate eigenvalue on these lines. In Regions I-III, the Hugoniot locus consists of three distinct lines, while in Region IV it consists of one line. Specifically, the boundary between Regions I and II is given by $a = \frac{3}{4} b^2$, the boundary between Regions II and III is given by $a = 1 + b^2$, and

the boundary between Regions III and IV is given by $4\{4b^2 - 3(a - 2)\}^3 = \{16b^3 + 9(1 - 2a)b\}^2$ [cf. 17]. The structure of solutions in each region is simplest when $b = 0$ since then solutions have both up-down symmetry [$(u,-v)$ satisfies (3) if and only if (u,v) does] and left-right symmetry [$(u(x,t),v(x,t))$ satisfies (3) if and only if $(-u(-x,t),v(-x,t))$ does]. We call the systems with $b = 0$ symmetric. (An additional simplifying feature of the symmetric systems is that the lines on which genuine nonlinearity fails coincide with the Hugoniot locus of the origin.)

The present paper is the first of a series in which we give the solution of the Riemann problem

$$\underset{\sim}{u}(x,0) = \begin{cases} \underset{\sim}{u}_L \equiv (u_L, v_L), & x < 0 \\ \underset{\sim}{u}_R \equiv (u_R, v_R), & x > 0 \end{cases} \tag{4}$$

for the symmetric systems in Regions II-IV of Schaeffer and Shearer [17]. There are new features in these regions that do not occur in Region I [cf. 18]. First, a type of shock which we call compressive appears in solutions of the Riemann problem, and the existence of such shocks is necessary to ensure (in the x,t-plane) the continuous dependence of solutions on $\underset{\sim}{u}_L$ and $\underset{\sim}{u}_R$ [cf. 6,7,9,21]. Schaeffer [25] noted that the compressive shocks perturb to a 1-shock followed by a 2-shock. This fact is manifested in the triple shocks which appear in the solutions.

A second feature that occurs in Regions II-IV that does not occur in Region I is the following: in Regions II-IV there are lines on which $\lambda = 0$, whereas in Region I, $\lambda = 0$ if and only if $\underset{\sim}{u} = 0$. These lines play a central role both in the classification as well as in the structure of Riemann problem solutions. In fact, the lines $\lambda = 0$ give a geometric interpretation for the boundaries between the Regions I-III located by Schaeffer and Shearer. (See the Appendix and Figure 8.) Also, in Regions II-IV the structure of the shock types on the Hugoniot locus of a point $\underset{\sim}{u}$ changes as $\underset{\sim}{u}$ crosses a line $\lambda = 0$; this entails a corresponding change in the structure of the solutions of the Riemann problem. The reason for the change in shock type is that the state $\underset{\sim}{u}$ on the line $\lambda = 0$ can be joined to the state $-\underset{\sim}{u}$ by a two-sided contact discontinuity.

Our construction of the solutions of the Riemann problem is based on a numerical construction of the Hugoniot loci together with the structure of the integral curves obtained from [17]. Some analysis is presented to justify the salient features of the solutions obtained. In particular, our analysis uses an explicit parameterization of the Hugoniot locus (see the Appendix). The fact that the Hugoniot locus is star-like with respect to the left state was pointed out by Shearer [24].

In the present paper we give the solution of the Riemann problem for system (3) in the parameter range

$$a > 2, \quad b = 0 . \tag{5}$$

This condition specifies the symmetric systems in Region IV. We present the solution in Section 3 by means of a series of diagrams (Figures 7A-F). Because of up-down symmetry, we give the solutions only for $\underset{\sim}{u}_L$ in the lower half-plane. The solution diagrams are qualitatively the same for all $\underset{\sim}{u}_L$ in the sector

$$A_1 = \{\underset{\sim}{u} : \theta_* < \theta_L < 0\} ,$$

and are qualitatively the same for all $\underset{\sim}{u}_L$ in the sector

$$A_2 = \{\underset{\sim}{u} : -\pi < \theta_L < \theta_*\} ,$$

where

$$\theta_L = \arctan\left(\frac{v_L}{u_L}\right) ,$$

$$\theta_* = \arctan(-\sqrt{a}) .$$

This separation angle θ_* depends on a, and the ray $\theta = \theta_*$ is the ray (in the lower half-plane) on which $\lambda_1 = 0$. The solution consists of a 1-composite wave followed by a 2-composite wave in analogy with the local solutions for strictly hyperbolic systems [cf. 11,14]. Here, however, the wave curves have a different structure: as in [6,7,9,21], intermediate solution states do not depend continuously on the data due to the appearance of compressive shocks. However, as in [6,7,9,21], continuous dependence on $\underset{\sim}{u}_L$ and $\underset{\sim}{u}_R$ is ensured in x,t-space because of the coincidence of shock speeds in the compressive

shocks. In this paper we construct explicitly for each state $\underset{\sim}{u}$ the 1-wave curve $W_1(\underset{\sim}{u})$ and the 2-wave curve $W_2(\underset{\sim}{u})$ such that the following theorem holds:

THEOREM: For each pair of states $\underset{\sim}{u}_L$ and $\underset{\sim}{u}_R$, there exists an intermediate state $\underset{\sim}{u}_M \in W_1(\underset{\sim}{u}_L)$ such that $\underset{\sim}{u}_R \in W_2(\underset{\sim}{u}_M)$ and the solution of the Riemann problem (3), (4), (5) consists of the 1-wave from $\underset{\sim}{u}_L$ to $\underset{\sim}{u}_M$ followed by the 2-wave from $\underset{\sim}{u}_M$ to $\underset{\sim}{u}_R$. Moreover, the solution is unique in x,t-space and depends continuously on $\underset{\sim}{u}_L$ and $\underset{\sim}{u}_R$.

In Figures 7A-F, pictorial solutions of the Riemann problem are presented in which the state $\underset{\sim}{u}_L$ is fixed, and an arbitrary point in the diagram represents $\underset{\sim}{u}_R$. The waves in the solution of the Riemann problem are determined by the path from $\underset{\sim}{u}_L$ to $\underset{\sim}{u}_R$ which consists of (portions of) wave curves and is indicated by the arrows.

In Section 2 we discuss the wave curves W_1 and W_2. In Section 3 we describe the diagrams in Figures 7A-E individually, and in Section 4 we verify the salient features of these diagrams. General properties of system (1) are stated in the Appendix and are referred to throughout. The Appendix also contains the interpretation of Regions I-III in terms of the lines $\lambda = 0$. These are depicted in Figures 8A-D.

§2. Elementary Waves

The integral curves of the eigenvector fields of the Jacobian $A(\underset{\sim}{u})$ determine the rarefaction waves of system (2). The Hugoniot loci $H(\underset{\sim}{u}_L)$ for states $\underset{\sim}{u}_L$ determine the shock waves of system (2), and are given by [20]

$$H(\underset{\sim}{u}_L) \equiv \{\underset{\sim}{u} : s(\underset{\sim}{u} - \underset{\sim}{u}_L) = \underset{\sim}{f}(\underset{\sim}{u}) - \underset{\sim}{f}(\underset{\sim}{u}_L) \quad \text{for some} \quad s \in \mathbf{R}\} .$$

The general solution of the Riemann problem which we construct is obtained by composing rarefaction waves and shock waves. Because the flux functions in (1) are homogeneous quadratics, the integral curves and Hugoniot loci for system (1) have the following scaling property: if Γ is an integral curve or Hugoniot locus through $\underset{\sim}{u}_L$, then $c\Gamma$ is the corresponding integral curve or Hugoniot locus through $c\underset{\sim}{u}_L$, $c \neq 0$. The eigenvalues and shock speeds scale similarly. Thus the integral curves and Hugoniot locus through $\underset{\sim}{u}_L$ determine the corresponding integral curves and Hugoniot locus for each state $\underset{\sim}{u}$ satisfying $\theta = \theta_L$ where

$$\theta = \arctan\left(\frac{v}{u}\right) .$$

For the Hugoniot loci, the up-down and left-right symmetries imply that if $\underset{\sim}{u}_R \in H(\underset{\sim}{u}_L)$, then $\bar{\underset{\sim}{u}}_R \in H(\bar{\underset{\sim}{u}}_L)$ and $\hat{\underset{\sim}{u}}_R \in H(\hat{\underset{\sim}{u}}_L)$ where $\bar{\underset{\sim}{u}} = (u,-v)$ and $\hat{\underset{\sim}{u}} = (-u,v)$. Thus, the reflection of a Hugoniot curve about either the u- or v-axis is also a Hugoniot curve. In terms of wave speeds and shock speeds, the symmetries of (3) when $b = 0$ yield the following relationships:

$$\lambda_p(\underset{\sim}{u}) = \lambda_p(\bar{\underset{\sim}{u}}) = -\lambda_{\hat{p}}(\hat{\underset{\sim}{u}}), \quad p = 1,2 \tag{2.1}$$

$$\sigma(\underset{\sim}{u}_L,\underset{\sim}{u}_R) = \sigma(\bar{\underset{\sim}{u}}_L,\bar{\underset{\sim}{u}}_R) = \sigma(\hat{\underset{\sim}{u}}_L,\hat{\underset{\sim}{u}}_R) \tag{2.2}$$

where $\hat{p}$ denotes the other family.

In Table 1 we label nine types of shocks according to the inequalities that hold between the characteristic speeds of $\underset{\sim}{u}_L$, $\underset{\sim}{u}_R$ and the shock speed $\sigma(\underset{\sim}{u}_L,\underset{\sim}{u}_R)$. (Obvious inequalities are omitted.) Since the two wave speeds λ_1 and λ_2 assigned to each state are ordered, Table 1 gives the totality of shock types that can occur in any 2×2 system (2). In the case of the symmetric systems (3), the formulas (2.1) and (2.2) imply the following symmetries for shock types: if $\underset{\sim}{u}_R \in H(\underset{\sim}{u}_L)$, then the shock type of

$\langle \bar{\underset{\sim}{u}}_L, \bar{\underset{\sim}{u}}_R \rangle$ will be the same as the shock type of $\langle \underset{\sim}{u}_L, \underset{\sim}{u}_R \rangle$; and the shock type of $\langle \hat{\underset{\sim}{u}}_L, \hat{\underset{\sim}{u}}_R \rangle$ will be what we call the inverse of the shock type of $\langle \underset{\sim}{u}_L, \underset{\sim}{u}_R \rangle$. Here, the inverse shock type is obtained by reversing the inequalities which hold between the shock speed and each wave speed to the right and left of the shock and also by interchanging the families 1 and 2. Therefore [cf. Table 1], 1-shock and 2-expansive are inverses; 2-shock and 1-expansive are inverses; compressive and expansive are inverses; right transport and left transport are inverses; and crossing is its own inverse. Thus in the symmetric cases, all Hugoniot curves and shock types are determined by the Hugoniot curves and shock types for states in a single quadrant of the u,v-plane. Among the above shock types, some occur in the solutions of system (3) that do not occur for strictly hyperbolic systems. For the symmetric systems of classes II-IV, there are three types of shocks that appear in solutions: 1-shocks, 2-shocks, and compressive shocks which are defined by [cf. Table 1]

$$\lambda_1(\underset{\sim}{u}_R) < \lambda_2(\underset{\sim}{u}_R) < \sigma(\underset{\sim}{u}_L, \underset{\sim}{u}_R) < \lambda_1(\underset{\sim}{u}_L) < \lambda_2(\underset{\sim}{u}_L) \ .$$

We refer to any of the three types of shocks above as admissible. We refer to shocks of other types as inadmissible. (We note that the transport shocks are the only types that do not appear in Hugoniot loci of the symmetric systems in classes II-IV.) Our scheme for labeling shock types in Figures 3-7 is described in the legend which precedes the diagrams.

1-SHOCK:	$s < \lambda_1(\underset{\sim}{u}_L)$ $\lambda_1(\underset{\sim}{u}_R) < s < \lambda_2(\underset{\sim}{u}_R)$	
1-EXPANSIVE:	$\lambda_1(\underset{\sim}{u}_L) < s < \lambda_2(\underset{\sim}{u}_L)$ $s < \lambda_1(\underset{\sim}{u}_R)$	
2-SHOCK:	$\lambda_1(\underset{\sim}{u}_L) < s < \lambda_2(\underset{\sim}{u}_L)$ $\lambda_2(\underset{\sim}{u}_R) < s$	
2-EXPANSIVE:	$\lambda_2(\underset{\sim}{u}_L) < s$ $\lambda_1(\underset{\sim}{u}_R) < s < \lambda_2(\underset{\sim}{u}_R)$	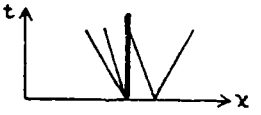
COMPRESSIVE:	$\lambda_2(\underset{\sim}{u}_R) < s < \lambda_1(\underset{\sim}{u}_L)$	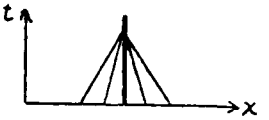
EXPANSIVE:	$\lambda_2(\underset{\sim}{u}_L) < s < \lambda_1(\underset{\sim}{u}_R)$	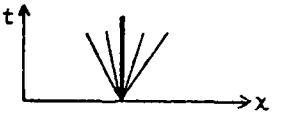
CROSSING:	$\lambda_1(\underset{\sim}{u}_L) < s < \lambda_2(\underset{\sim}{u}_L)$ $\lambda_1(\underset{\sim}{u}_R) < s < \lambda_2(\underset{\sim}{u}_R)$	
RIGHT TRANSPORT:	$s < \lambda_1(\underset{\sim}{u}_L)$ $s < \lambda_1(\underset{\sim}{u}_R)$	
LEFT TRANSPORT:	$\lambda_2(\underset{\sim}{u}_L) < s$ $\lambda_2(\underset{\sim}{u}_R) < s$	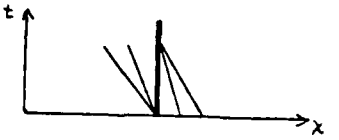

TABLE 1

In the diagrams above, the centerline denotes a shock in x,t-space. The lines to the left and right of the shock are characteristic lines, and indicate the relationship between the shock speed and the wave speeds on the left and right.

§2.1. Integral Curves

For system (3) with parameter values (5),

$$A(\underset{\sim}{u}) = \begin{bmatrix} au & v \\ v & u \end{bmatrix} ,$$

and the integral curves are depicted in Figure 1 [3,17]. We call the integral curves associated with the eigenvalues $\lambda_1(\underset{\sim}{u}) < \lambda_2(\underset{\sim}{u})$ the 1-, 2-integral curves. For example, when $a = 3$ the integral curves are the one-parameter family of parabolas

$$u - u_0 = -\frac{1}{4u_0} v^2 ,$$

where u_0 is the value at which the parabola crosses the u-axis. The u-axis is itself an integral curve for the symmetric systems $b = 0$. For general $a > 2$, the integral curves are parabola-like and the 1-integral curves open to the left, the 2-integral curves open to the right. The arrows in Figure 1 indicate the direction in which the corresponding eigenvalues increase. We define the i-rarefaction curve $R_i(\underset{\sim}{u}_L)$, $i = 1,2$, to be the set of states $\underset{\sim}{u}_R$ such that the solution of the Riemann problem (3), (4) is a pure i-rarefaction wave (see [14]); $R_i(\underset{\sim}{u}_L)$ is thus the connected portion of the i-integral curve through $\underset{\sim}{u}_L$ consisting of those states $\underset{\sim}{u}$ for which λ_i increases along the curve from $\underset{\sim}{u}_L$ to $\underset{\sim}{u}$.

§2.2. The Hugoniot Locus

For system (3) with parameter values (5), the qualitative shape of the Hugoniot locus $H(\underset{\sim}{u}_L)$ is as follows: for $\underset{\sim}{u}_L = \underset{\sim}{0}$, $H(\underset{\sim}{u}_L)$ is the u-axis; for $\underset{\sim}{u}_L$ on the u-axis, $H(\underset{\sim}{u}_L)$ consists of an ellipse together with the u-axis; and for $\underset{\sim}{u}_L$ off the u-axis, $H(\underset{\sim}{u}_L)$ perturbs to a closed loop surrounding the origin with two tails which are asymptotic at infinity to opposite ends of the horizontal line

$$v = \frac{a}{a-2} v_L .$$

These properties follow from the explicit parameterization of the Hugoniot locus given in the Appendix and are depicted in Figures 3A-F. The shock type is also indicated. We

let $S_p(\underset{\sim}{u}_L)$ denote that portion of $H(\underset{\sim}{u}_L)$ consisting of 1-shocks for $p = 1$, 2-shocks for $p = 2$, and compressive shocks for $p = c$.

The subset $S_c(\underset{\sim}{u}_L)$ is non-empty for $\underset{\sim}{u}_L$ in the sector A_1, and $S_c(\underset{\sim}{u}_L)$ is empty for $\underset{\sim}{u}_L$ in the sector A_2. Moreover, $S_1(\underset{\sim}{u}_L)$ has two disconnected components for $\underset{\sim}{u}_L \in A_1$ but only one for $\underset{\sim}{u}_L \in A_2$. This explains why the ray $\theta = \theta_*$ is the boundary across which the qualitative structure of the solution diagrams changes.

We note in Figure 3B that B_L, D_L are the points at which

$$\sigma(\underset{\sim}{u}_L, B_L) = \lambda_1(\underset{\sim}{u}_L) = \sigma(\underset{\sim}{u}_L, D_L) ;$$

in Figures 3A, B, C, D that C_L is the point at which

$$\lambda_2(C_L) = \sigma(\underset{\sim}{u}_L, C_L) ;$$

and in Figure 3C that

$$\lambda_1(\underset{\sim}{u}_L) = \sigma(\underset{\sim}{u}_L, C_L) = \lambda_2(C_L) \quad (= 0) .$$

§2.3. Composite Waves

The solutions of the Riemann problem are compositions of pure rarefaction waves and pure shock waves. We refer to a Riemann problem solution consisting entirely of waves of one family as a composite wave of that family. The composite waves in the solutions of Riemann problems for system (3) in parameter range (5) are of two types: a 1-rarefaction wave followed by a 1-shock wave and a 2-shock wave followed by a 2-rarefaction wave. In each case, the speed of the shock equals the speed of the adjacent rarefaction wave. We call these 1RS- and 2SR-composite waves, respectively. (See Figure 4. The letters in Figure 4 refer to states appearing in Figure 5 where the composite waves may be viewed in state space.)

For each $\underset{\sim}{u}$ we define the 1-composite curve $C_1(\underset{\sim}{u})$. In Figure 5 a 1RS-composite wave with left state $\underset{\sim}{u}$ is a wave consisting of a 1-rarefaction wave from $\underset{\sim}{u}$ to $F \in R_1(\underset{\sim}{u})$ followed by a 1-shock from F to $D \in S_1(F)$ such that $\sigma(F,D) = \lambda_1(F)$. Such a shock exists if and only if F lies on that portion of $R_1(\underset{\sim}{u})$ in Sector A_1. We define the 1-composite curve $C_1(\underset{\sim}{u})$ to be the set of all such states D. Thus, the 1-

composite curve $C_1(\underset{\sim}{u}_*)$ is maximal for $\underset{\sim}{u}_*$ on the boundary ray $\theta = \theta_*$ in the sense that

$$C_1(\underset{\sim}{u}_*) = C_1(\underset{\sim}{u}) \quad \text{for} \quad \underset{\sim}{u}_* \in R_1(\underset{\sim}{u}) ,$$

$$C_1(\underset{\sim}{u}_*) \supseteq C_1(\underset{\sim}{u}) \quad \text{for} \quad \underset{\sim}{u} \in R_1(\underset{\sim}{u}_*) ;$$

for example, in Figure 5,

$$C_1(\underset{\sim}{u}) = C_1(\underset{\sim}{u}_*) = [EDC_*] \quad \text{and} \quad C_1(F) = [ED] \subseteq C_1(\underset{\sim}{u}_*) .$$

(Here, letters enclosed by brackets denote the curves that connect the corresponding points in the Figures.) In fact, as F moves from E to $\underset{\sim}{u}_*$ along $R_1(\underset{\sim}{u}_*)$, D moves from E to C_* along $C_1(\underset{\sim}{u}_*)$. Moreover,

$$C_* = -\underset{\sim}{u}_* ,$$

and

$$\sigma(\underset{\sim}{u}_*, C_*) = \lambda_2(C_*) = \lambda_1(\underset{\sim}{u}_*) = 0 .$$

For each curve Γ we define the 2-boundary curve based on Γ. In Figure 5, a 2SR-composite wave with left state $\underset{\sim}{u}$ is a wave consisting of a 2-shock wave from $\underset{\sim}{u}$ to $C \in S_2(\underset{\sim}{u})$ followed by a 2-rarefaction wave from C to any $G \in R_2(C)$ such that $\sigma(\underset{\sim}{u}, C) = \lambda_2(C)$. *Such a shock exists if and only if* $\underset{\sim}{u}$ lies on that portion of Γ in sector A_2. We define the 2-boundary curve to be the set of all such states C. For example, in Figure 5, $[C_*C^\infty]$ is the 2-boundary curve based on $[\underset{\sim}{u}_*\underset{\sim}{u}^\infty]$. Thus, for left states $\underset{\sim}{u}$ on $\Gamma = [\underset{\sim}{u}_*\underset{\sim}{u}^\infty]$, the states C on the 2-boundary curve $[C_*C^\infty]$ are transition states between 2-shock waves and 2-composite waves.

§2.4. Wave Curves

We define the wave curve $W_i(\underset{\sim}{u}_L)$, i = 1,2, to be the set of states $\underset{\sim}{u}_R$ for which the solution of the Riemann problem (2), (4) is a pure composite wave of the appropriate family. Thus, (see Figures 6A, B)

$$W_1(\underset{\sim}{u}_L) = S_1(\underset{\sim}{u}_L) \cup R_1(\underset{\sim}{u}_L) \cup C_1(\underset{\sim}{u}_L) ,$$

and

$$W_2(\underset{\sim}{u}_L) = R_2(\underset{\sim}{u}_L) \cup S_2(\underset{\sim}{u}_L) \cup R_2(C) ,$$

where C is the endpoint of $S_2(\underset{\sim}{u}_L)$ at which $\sigma(\underset{\sim}{u}_L, C) = \lambda_2(C)$. The geometry of these curves is indicated in Figure 6 for $\underset{\sim}{u}_L$ in sectors A_1 and A_2.

§3. Solution of the Riemann Problem

For each $\underset{\sim}{u}_L$ we describe the solution of the Riemann problem for arbitrary $\underset{\sim}{u}_R$ by means of a diagram. In Figures 7B and D we present a diagram of the solution of the Riemann problem for representative values of $\underset{\sim}{u}_L$ in sectors A_1 and A_2 in each of which the solution diagrams are qualitatively the same. For completeness and in order to see clearly the continuous dependence of solutions on $\underset{\sim}{u}_L$, we also give in Figures 7A,C,E the solution diagrams for typical values of $\underset{\sim}{u}_L$ on the boundaries of sectors A_1 and A_2, i.e., for $\underset{\sim}{u}_L$ on the rays $\theta = 0$, $\theta = \theta_*$, and $\theta = -\pi$. In Figures 7A-D, the representative values $\underset{\sim}{u}_L$ are chosen to lie on the 1-integral curve through the fixed state E on the positive u-axis. In Figure 7F we present the solution for $\underset{\sim}{u}_L = \underset{\sim}{0}$.

The solution of the Riemann problem consists of a 1-wave with left state $\underset{\sim}{u}_L$ and right state $\underset{\sim}{u}_M$ followed by a 2-wave with left state $\underset{\sim}{u}_M$ and right state $\underset{\sim}{u}_R$. We find the intermediate state in the Figures as follows: given $\underset{\sim}{u}_R$, follow the 2-wave curve backwards from $\underset{\sim}{u}_R$ (opposite the direction of the arrows) until you reach a point $\underset{\sim}{u}_M$ in the 1-wave curve $W_1(\underset{\sim}{u}_L)$. The state $\underset{\sim}{u}_M$ so constructed satisfies $\underset{\sim}{u}_R \in W_2(\underset{\sim}{u}_M)$ and defines the waves in the solution. This procedure is not well-defined when $\{\underset{\sim}{u}_L, \underset{\sim}{u}_M, \underset{\sim}{u}_R\}$ form a triple shock:

$$u_M \in H(\underset{\sim}{u}_L),\ \underset{\sim}{u}_R \in H(\underset{\sim}{u}_L),\ u_R \in H(\underset{\sim}{u}_M)\ , \tag{3.1}$$

and

$$\sigma(\underset{\sim}{u}_L, \underset{\sim}{u}_M) = \sigma(\underset{\sim}{u}_L, \underset{\sim}{u}_R) = \sigma(\underset{\sim}{u}_M, \underset{\sim}{u}_R)\ . \tag{3.2}$$

Triple shocks occur when $\underset{\sim}{u}_R \in S_c(\underset{\sim}{u}_L)$ or when $\underset{\sim}{u}_R$ is in the triple shock curve (which will be defined in each Figure). When the procedure is not well-defined, there are two such intermediate states $\underset{\sim}{u}_M$; however, the two solutions obtained are identical in x,t-space because then all shock speeds in the problem are equal. This ensures continuous dependence of the solution on the initial data $\underset{\sim}{u}_L$ and $\underset{\sim}{u}_R$.

We now discuss the solution diagrams 7A-E individually.

§3.1. Solution for $\theta_L = 0$

In Figure 7A, $\underset{\sim}{u}_L \equiv E$ lies on the u-axis to the right of the origin. In this case the Hugoniot locus $H(\underset{\sim}{u}_L)$ consists of the u-axis together with the ellipse $\mathcal{E}$ depicted. The vertices of $\mathcal{E}$ on the major axis are $\underset{\sim}{u}_L$ and $C_L \equiv -\frac{a}{a-2}\underset{\sim}{u}_L$. The point A is given by

$$A = -\frac{a-2}{a}\underset{\sim}{u}_L \,. \tag{3.3}$$

Point A is the limit of intersections of $S_2(\underset{\sim}{u})$ with the u-axis as $\underset{\sim}{u}$ tends to $\underset{\sim}{u}_L$ through states with $v \neq 0$. The solution of the Riemann problem consists of a 1-shock with left state $\underset{\sim}{u}_L$ and right state $\underset{\sim}{u}_M \in S_1(\underset{\sim}{u}_L)$ followed by a 2-rarefaction wave if $\underset{\sim}{u}_R$ lies outside $\mathcal{E}$, and followed by a 2-shock if $\underset{\sim}{u}_R$ lies inside $\mathcal{E}$. The u-axis between C_L and A is $S_c(\underset{\sim}{u}_L)$ where triple shocks occur in pairs. In fact, for each $\underset{\sim}{v} \in \mathcal{E}$, $v \neq \underset{\sim}{u}_L$, there exists a unique $\underset{\sim}{y} \in S_c(\underset{\sim}{u}_L)$ such that both $\{\underset{\sim}{u}_L, \underset{\sim}{v}, \underset{\sim}{y}\}$ and $\{\underset{\sim}{u}_L, \bar{\underset{\sim}{v}}, \underset{\sim}{y}\}$ are triple shocks of the same speed. (Here $\bar{\underset{\sim}{v}}$ is the reflection of $\underset{\sim}{v}$ in the u-axis.) Thus for $\underset{\sim}{u}_R \in S_c(\underset{\sim}{u}_L)$, the solution of the Riemann problem is unambiguous in the x,t-plane.

§3.2. Solution for $\theta_* < \theta_L < 0$

In Figure 7B, $\underset{\sim}{u}_L$ lies in the sector A_1. The Hugoniot locus $H(\underset{\sim}{u}_L)$ is depicted by the thin solid curve through $\underset{\sim}{u}_L$. Here

$$S_1(\underset{\sim}{u}_L) = [\infty K_L \underset{\sim}{u}_L] \cup [D_L C_L] \,,$$

$$R_1(\underset{\sim}{u}_L) = [\underset{\sim}{u}_L E] \,,$$

$$C_1(\underset{\sim}{u}_L) = [E D_L] \,,$$

and the union of these three curves is the 1-wave curve $W_1(\underset{\sim}{u}_L)$. Moreover,

$$S_c(\underset{\sim}{u}_L) = [C_L B_L] \,,$$

and the triple shock curve is $[B_L A]$.

For $\underset{\sim}{u}_R$ on either of these latter two curves, triple shocks occur: for $R \in S_c(\underset{\sim}{u}_L)$ there is a pair of triple shocks $\{\underset{\sim}{u}_L, P, R\}$ and $\{\underset{\sim}{u}_L, Q, R\}$ with all shock

speeds being equal; for $R \in [B_L A]$, a single triple shock occurs. Hence, continuous dependence is ensured.

The curve $[C_L C'^{\infty}]$ is the 2-boundary curve based on $[K_L \underset{\sim}{u}'^{\infty}]$, and 2SR-composite waves occur precisely when $\underset{\sim}{u}_R$ lies "above" $[C_L C'^{\infty}]$ so that $\underset{\sim}{u}_M \in [K_L \underset{\sim}{u}'^{\infty}]$.

The states B_L and D_L satisfy

$$\sigma(\underset{\sim}{u}_L, B_L) = \sigma(\underset{\sim}{u}_L, D_L) = \sigma(D_L, B_L) = \lambda_1(\underset{\sim}{u}_L) \ .$$

The state C_L is the point where $H(\underset{\sim}{u}_L)$ is tangent to a 2-integral curve. (See the Tangency Rule in the Appendix.) This implies that $\sigma(\underset{\sim}{u}_L, C_L) = \lambda_2(C_L)$ and that C_L is in, and marks the end of, the 2-boundary curve $[C_L C'^{\infty}]$. This insures continuous dependence near the point C_L.

For $\underset{\sim}{u}_L$ in sector A_1, the states B_L, D_L separate the states $\underset{\sim}{u}_L$, C_L on the portion of $H(\underset{\sim}{u}_L)$ consisting of the closed loop. As θ_L decreases to θ_*, B_L and D_L become coincident with C_L, and so both $S_c(\underset{\sim}{u}_L)$ and the disconnected portion $[D_L C_L]$ of $S_1(\underset{\sim}{u}_L)$ disappear. The fact that there exists a point at which $H(\underset{\sim}{u}_L)$ intersects the 1-composite curve $[ED_L]$ characterizes the states in A_1.

§3.3. Solution for $\theta_L = \theta_*$

In Figure 7C, $\underset{\sim}{u}_L = \underset{\sim}{u}_*$ lies on the line $\theta = \theta_*$. The Hugoniot locus $H(\underset{\sim}{u}_L)$ is depicted by the thin solid curve through $\underset{\sim}{u}_L$. Here

$$S_1(\underset{\sim}{u}_L) = [\infty \underset{\sim}{u}' \underset{\sim}{u}_L] \ ,$$

$$R_1(\underset{\sim}{u}_L) = [\underset{\sim}{u}_L E] \ ,$$

and

$$C_1(\underset{\sim}{u}_L) = [ED_L] \ .$$

The union of these three curves is $W_1(\underset{\sim}{u}_L)$. In this case

$$S_c(\underset{\sim}{u}_L) = \{C_*\} \ ,$$

and the curve $[C_* A]$ is the triple shock curve.

The curve $[C_* C'^{\infty}]$ is the 2-boundary curve based on $[\underset{\sim}{u}_L \underset{\sim}{u}'^{\infty}]$, and 2SR-composite waves occur precisely when $\underset{\sim}{u}_R$ lies "above" $[C_* C'^{\infty}]$ so that $\underset{\sim}{u}_M \in [\underset{\sim}{u}_L \underset{\sim}{u}'^{\infty}]$. Note that

$C_* = -\underset{\sim}{u}_L$ is the point where $H(\underset{\sim}{u}_L)$ is tangent to a 2-rarefaction curve, and also that

$$\sigma(\underset{\sim}{u}_L, C_*) = \lambda_1(\underset{\sim}{u}_L) = \lambda_2(C_*) \ .$$

Thus $\theta = \theta_*$ is the ray where B_L, C_L and D_L are coincident.

§3.4. Solution for $-\pi < \theta_L < \theta_*$

In Figure 7D, $\underset{\sim}{u}_L$ lies in sector A_2. The Hugoniot locus $H(\underset{\sim}{u}_L)$ is depicted by the thin solid curve through $\underset{\sim}{u}_L$. Here

$$S_1(\underset{\sim}{u}_L) = [\infty\underset{\sim}{u}'\underset{\sim}{u}_L] \ ,$$

$$R_1(\underset{\sim}{u}_L) = [\underset{\sim}{u}_L FE] \ ,$$

and

$$C_1(\underset{\sim}{u}_L) = [EDC_*] \ .$$

The union of these three curves is $W_1(\underset{\sim}{u}_L)$. In this case

$$S_C(\underset{\sim}{u}_L) = \emptyset \ , \tag{3.4}$$

and $[ABC_*]$ is the triple shock curve. Condition (3.4) characterizes the states in A_2.

For $\underset{\sim}{u}_M \in [\underset{\sim}{u}_* EC_*]$, the solution consists of a 1-rarefaction wave taking $\underset{\sim}{u}_L$ to $\underset{\sim}{u}_*$ followed by the solution of the Riemann problem $\langle \underset{\sim}{u}_*, \underset{\sim}{u}_R \rangle$ given in Section 3.3. The curve $[C_* C_L^\infty]$ is the 2-boundary curve with base curve $[\infty\underset{\sim}{u}_L\underset{\sim}{u}_*]$, and again 2SR-composite waves occur precisely when $\underset{\sim}{u}_R$ lies "above" the curve $[C_* C_L^\infty]$ so that $\underset{\sim}{u}_M \in [\infty\underset{\sim}{u}_L\underset{\sim}{u}_*]$.

Note that C_* is the end of the 1-composite curve in the sense that there do not exist 1-shocks with left states $\underset{\sim}{u} \in [\underset{\sim}{u}_L\underset{\sim}{u}_*]$ which have speed $\lambda_1(\underset{\sim}{u})$.

§3.5. Solution for $\theta_L = -\pi$

In Figure 7E, $\underset{\sim}{u}_L$ lies on the negative u-axis. The Hugoniot locus consists of the u-axis together with the ellipse E depicted. The vertices of E on the major axis are $\underset{\sim}{u}_L$ and $G = -\left(\frac{a}{a-2}\right)\underset{\sim}{u}_L$, and

$$S_1(\underset{\sim}{u}_L) = [\infty\underset{\sim}{u}_L] \ ,$$

and

$$R_1(\underset{\sim}{u}_L) = [\underset{\sim}{u}_L 0] \ .$$

The union of these two curves is $W_1(\underset{\sim}{u}_L)$. Here

$$C_1(\underset{\sim}{u}_L) = S_c(\underset{\sim}{u}_L) = \phi \ ,$$

and the solution of the Riemann problem consists of a 1-wave followed by a 2-rarefaction wave. The solution for $\underset{\sim}{u}_L = \underset{\sim}{0}$ is similar and given in Figure 7F.

§4. Justification

The solution of the Riemann problem presented in Section 3 is based on the assumptions that the integral curves and Hugoniot loci have the qualitative features discussed in Section 2. The relevant features of the integral curves which are required for our analysis are verified in [3,17]. The features of $H(\underset{\sim}{u}_L)$ (including shapes and locations of shock types) have been verified numerically, using an explicit parameterization of $H(\underset{\sim}{u}_L)$ (see the Appendix). We here present analytical evidence which supports the results of these numerical computations. Note that for $\underset{\sim}{u}_L$ off the u-axis, system (3) in parameter range (5) is strictly hyperbolic and genuinely nonlinear in a neighborhood of $\underset{\sim}{u}_L$, and so the local theory of Lax [11] applies in some neighborhood of $\underset{\sim}{u}_L$. We now discuss the global features of the Hugoniot loci depicted in Figures 3A-C.

Figure 3A: In this case $\underset{\sim}{u}_L$ is on the positive u-axis. The Hugoniot locus $H(\underset{\sim}{u}_L)$ consists of the u-axis together with the ellipse E given by

$$(a - 2)u^2 + 2u_L u + v^2 = au_L^2 ,$$

with center $-\frac{1}{(a-2)}\underset{\sim}{u}_L$. For $\underset{\sim}{u} = (u,0)$, we have (see the Appendix)

$$\sigma(\underset{\sim}{u}_L,\underset{\sim}{u}) = \frac{1}{2}a(u + u_L) ,$$

$$\{\lambda_1(\underset{\sim}{u}),\lambda_2(\underset{\sim}{u})\} = \{au,u\} \text{ and } \{\lambda_1(\underset{\sim}{u}_L),\lambda_2(\underset{\sim}{u}_L)\} = \{au_L,u_L\} ,$$

which verifies the shock types on the axis, and verifies that the shock type changes at

$$\underset{\sim}{u}_L,\ C_L \equiv -\frac{a}{a-2}\underset{\sim}{u}_L, \text{ and } A \equiv -\frac{a-2}{a}\underset{\sim}{u}_L .$$

Figure 3B: In this case $\underset{\sim}{u}_L \in A_1$. The points B_L, C_L and D_L are points where a transition in shock type occurs. The existence of the point C_L where $H(\underset{\sim}{u}_L)$ is tangent to a 2-integral curve follows from the geometry of the integral curves. This tangency at C_L implies (see the Tangency Rule in the Appendix)

$$\lambda_2(C_L) = \sigma(\underset{\sim}{u}_L,C_L) .$$

Note also that $\bar{\underset{\sim}{u}}_L$ and $-\underset{\sim}{u}_L$ both lie on $H(\underset{\sim}{u}_L)$, and

$$\sigma(\underset{\sim}{u}_L,\bar{\underset{\sim}{u}}_L) = u_L ,$$

$$\sigma(\underset{\sim}{u}_L, -\underset{\sim}{u}_L) = 0 \ .$$

This is obtained from the Midpoint Rule or directly from the Rankine-Hugoniot condition (see the Appendix). Also the speed $\lambda_1(\underset{\sim}{u}_L)$ satisfies

$$0 < \lambda_1(\underset{\sim}{u}_L) = \frac{a+1}{2} u_L - \frac{1}{2}\sqrt{(a-1)^2 u_L^2 + 4v_L^2} < u_L = \sigma(\underset{\sim}{u}_L, \bar{\underset{\sim}{u}}_L) \ ,$$

where the left hand inequality is equivalent to $\underset{\sim}{u} \in A_1$. Thus the shock speed $\sigma(\underset{\sim}{u}_L, \bar{\underset{\sim}{u}}_L)$ is larger than $\lambda_1(\underset{\sim}{u}_L)$, but $\sigma(\underset{\sim}{u}_L, -\underset{\sim}{u}_L)$ is smaller than $\lambda_1(\underset{\sim}{u}_L)$; hence, there exists a point $D_L \in H(\underset{\sim}{u}_L)$ between $\bar{\underset{\sim}{u}}_L$ and $-\underset{\sim}{u}_L$ at which $\sigma(\underset{\sim}{u}_L, D_L) = \lambda_1(\underset{\sim}{u}_L)$. Similarly,

$$\underset{\sim}{u}_0 \equiv \left(\frac{1}{a}\left\{u_L - \sqrt{(a-1)^2 u_L^2 + a v_L^2}\right\}, 0\right)$$

is the intersection of $H(\underset{\sim}{u}_L)$ with the negative u-axis, and satisfies (see Appendix)

$$\sigma(\underset{\sim}{u}_L, \underset{\sim}{u}_0) = u_L \ .$$

Therefore, there is a point B_L above the u-axis between $-\underset{\sim}{u}_L$ and $\underset{\sim}{u}_0$ at which $\sigma(\underset{\sim}{u}_L, B_L) = \lambda_1(\underset{\sim}{u}_L)$. Consequently, $\{\underset{\sim}{u}_L, B_L, D_L\}$ is a triple shock.

Figure 3C: In this case $\underset{\sim}{u}_L = \underset{\sim}{u}_*$ is on the ray $\theta = \theta_*$. As θ_L decreases to θ_* in Figure 3B, $S_c(\underset{\sim}{u}_L)$ and the portion $[D_L C_L] \subseteq S_1(\underset{\sim}{u}_L)$ vanish. In fact,

$$\lambda_1(\underset{\sim}{u}_*) = \sigma(\underset{\sim}{u}_*, -\underset{\sim}{u}_*) = \lambda_2(-\underset{\sim}{u}_*) = 0 \ ,$$

indicating that the points B_L and D_L do indeed become coincident with $-\underset{\sim}{u}_*$ as θ_L decreases to θ_*. We also note that $\lambda_2(-\underset{\sim}{u}_*) = \sigma(\underset{\sim}{u}_*, -\underset{\sim}{u}_*)$ implies, by the Tangency Rule, that $H(\underset{\sim}{u}_*)$ is tangent to a 2-integral curve at $-\underset{\sim}{u}_*$ and thus $C_L = -\underset{\sim}{u}_*$.

APPENDIX

Here we list for reference several properties of the quadratic conservation laws (1) which are helpful in the study of the Riemann problem.

MIDPOINT RULE: For system (1), $\underset{\sim}{u}_R \in H(\underset{\sim}{u}_L)$ if and only if the line segment joining $\underset{\sim}{u}_L$ to $\underset{\sim}{u}_R$ is tangent to a p-integral curve at the midpoint of the segment. Moreover, in this case

$$\sigma(\underset{\sim}{u}_L,\underset{\sim}{u}_R) = \lambda_p\left(\frac{\underset{\sim}{u}_L + \underset{\sim}{u}_R}{2}\right) . \tag{A.1}$$

Proof: Use the linearity of $\dfrac{\partial \underset{\sim}{f}}{\partial \underset{\sim}{u}}$ together with the general formula

$$s(\underset{\sim}{u}_R - \underset{\sim}{u}_L) = \underset{\sim}{f}(\underset{\sim}{u}_R) - \underset{\sim}{f}(\underset{\sim}{u}_L) = \left\{\int_0^1 \frac{\partial \underset{\sim}{f}}{\partial \underset{\sim}{u}}(\underset{\sim}{u}_L + \tau(\underset{\sim}{u}_R - \underset{\sim}{u}_L))d\tau\right\}\cdot(\underset{\sim}{u}_R - \underset{\sim}{u}_L) .$$

TRIPLE SHOCK RULE: For system (2), suppose the states $\underset{\sim}{u}_1$, $\underset{\sim}{u}_2$, and $\underset{\sim}{u}_3$ satisfy

$$\underset{\sim}{u}_1 \in H(\underset{\sim}{u}_2),\ \underset{\sim}{u}_2 \in H(\underset{\sim}{u}_3),\ \underset{\sim}{u}_3 \in H(\underset{\sim}{u}_1) . \tag{A.2}$$

Then either $\underset{\sim}{u}_1$, $\underset{\sim}{u}_2$ and $\underset{\sim}{u}_3$ are colinear or else

$$\sigma(\underset{\sim}{u}_2,\underset{\sim}{u}_1) = \sigma(\underset{\sim}{u}_3,\underset{\sim}{u}_2) = \sigma(\underset{\sim}{u}_1,\underset{\sim}{u}_3) . \tag{A.3}$$

Proof: Let $s_{ij} = \sigma(\underset{\sim}{u}_i,\underset{\sim}{u}_j)$. Then

$$s_{21}(\underset{\sim}{u}_2 - \underset{\sim}{u}_1) = \underset{\sim}{f}(\underset{\sim}{u}_2) - \underset{\sim}{f}(\underset{\sim}{u}_1) ,$$

$$s_{32}(\underset{\sim}{u}_3 - \underset{\sim}{u}_2) = \underset{\sim}{f}(\underset{\sim}{u}_3) - \underset{\sim}{f}(\underset{\sim}{u}_2) ,$$

$$s_{13}(\underset{\sim}{u}_1 - \underset{\sim}{u}_3) = \underset{\sim}{f}(\underset{\sim}{u}_1) - \underset{\sim}{f}(\underset{\sim}{u}_3) .$$

Adding gives

$$(s_{21} - s_{13})(\underset{\sim}{u}_2 - \underset{\sim}{u}_1) + (s_{32} - s_{13})(\underset{\sim}{u}_3 - \underset{\sim}{u}_2) = 0 ,$$

and the result follows.

TANGENCY RULE: For system (3), assume that $\underset{\sim}{u}_L \notin H(\underset{\sim}{0})$. Then the following statements are equivalent regarding $\underset{\sim}{u} \in H(\underset{\sim}{u}_L)$, $\underset{\sim}{u} \neq \underset{\sim}{u}_L$:

(i) $H(\underset{\sim}{u}_L)$ is tangent to a p-integral curve at the point $\underset{\sim}{u}$.

(ii) $\dot{s} = 0$ at $\underset{\sim}{u}$. (Dot denotes differentiation with respect to arc length along $H(\underset{\sim}{u}_L)$.)

(iii) $\lambda_p(\underset{\sim}{u}) = \sigma(\underset{\sim}{u}_L, \underset{\sim}{u})$.

Proof: Differentiate

$$s(\underset{\sim}{u} - \underset{\sim}{u}_L) = \underset{\sim}{f}(\underset{\sim}{u}) - \underset{\sim}{f}(\underset{\sim}{u}_L)$$

along $H(\underset{\sim}{u}_L)$ to obtain

$$\dot{s}(\underset{\sim}{u} - \underset{\sim}{u}_L) + s\dot{\underset{\sim}{u}} = A(\underset{\sim}{u})\dot{\underset{\sim}{u}} ,$$

or

$$[A(\underset{\sim}{u}) - sI]\dot{\underset{\sim}{u}} = \dot{s}(\underset{\sim}{u} - \underset{\sim}{u}_L) . \tag{A.4}$$

Suppose $H(\underset{\sim}{u}_L)$ is tangent to a p-integral curve. Then $\dot{\underset{\sim}{u}}$ is a right eigenvector of A with eigenvalue λ_p so that (A.4) becomes

$$(\lambda_p - s)\dot{\underset{\sim}{u}} = \dot{s}(\underset{\sim}{u} - \underset{\sim}{u}_L) . \tag{A.5}$$

Since $\underset{\sim}{u}_L \notin H(\underset{\sim}{0})$, the line joining $\underset{\sim}{u}_L$ to $\underset{\sim}{u}$ is not tangent to $H(\underset{\sim}{u}_L)$ at $\underset{\sim}{u}$. Thus we conclude from (A.5) that $\dot{s} = 0$ and $s = \lambda_p$, so that (i) => (ii) and (i) => (iii). Now suppose (ii). Then (A.4) gives that $\dot{\underset{\sim}{u}}$ is an eigenvector and $s = \lambda_p$ for $p = 1$ or 2. Thus (ii) => (i) and (ii) => (iii). Finally suppose (iii): $s = \lambda_p(\underset{\sim}{u})$. If $\dot{\underset{\sim}{u}}$ is not parallel to the eigenvector $\underset{\sim}{r}_p$ of $A(\underset{\sim}{u})$ *and* $\dot{s} \neq 0$ *then*, (A.4) implies that $\underset{\sim}{u} - \underset{\sim}{u}_L$ is parallel to $\underset{\sim}{r}_p$, (the other eigenvector of $A(\underset{\sim}{u})$). However, by the midpoint rule, $\underset{\sim}{u} - \underset{\sim}{u}_L$ is also tangent to an integral curve at $\frac{1}{2}(\underset{\sim}{u}_L + \underset{\sim}{u})$. But this contradicts the fact that if $\underset{\sim}{u}_L \notin H(\underset{\sim}{0})$, then every line through $\underset{\sim}{u}_L$ is tangent exactly once to an integral curve. Consequently, $\dot{\underset{\sim}{u}}$ is tangent to $\underset{\sim}{r}_p$ at $\underset{\sim}{u}$, and hence $\dot{s} = 0$. Thus (iii) => (i) and (iii) => (ii).

EIGENVALUES AND SHOCK SPEEDS: For system (3) with $b = 0$, the eigenvalues are

$$\lambda_{1,2}(\underset{\sim}{u}) = \frac{1}{2}\left\{(a + 1)u \pm \sqrt{(a - 1)^2u^2 + 4v^2}\right\} .$$

In addition, if $\underset{\sim}{u}_R \in H(\underset{\sim}{u}_L)$, then the Rankine-Hugoniot condition gives

$$\sigma(\underset{\sim}{u}_L, \underset{\sim}{u}_R) = \frac{u_R v_R - u_L v_L}{v_R - v_L} \quad (v_R \neq v_L) .$$

SPECIAL POINTS ON $H(\underset{\sim}{u}_L)$: For system (3) with $b = 0$,

$$-\underset{\sim}{u}_L \in H(\underset{\sim}{u}_L) \quad \text{with} \quad \sigma(\underset{\sim}{u}_L, -\underset{\sim}{u}_L) = 0 ,$$

and

$$\bar{\underset{\sim}{u}}_L \in H(\underset{\sim}{u}_L) \quad \text{with} \quad \sigma(\underset{\sim}{u}_L, \bar{\underset{\sim}{u}}_L) = u_L .$$

Moreover, $H(\underset{\sim}{u}_L)$ crosses the u-axis at the points

$$\underset{\sim}{u} \equiv \left(\frac{1}{a}\left\{u_L \pm \sqrt{(a-1)^2 u_L^2 + a v_L^2}\right\}, 0\right) ,$$

and for such values of $\underset{\sim}{u}$,

$$\sigma(\underset{\sim}{u}_L, \underset{\sim}{u}) = u_L$$

when $(a-1)^2 u_L^2 + a v_L^2 > 0$.

PARAMETRIZATION OF $H(\underset{\sim}{u}_L)$: For system (1), the Hugoniot locus $H(\underset{\sim}{u}_L)$ for $\underset{\sim}{u}_L \notin H(\underset{\sim}{0})$ is parametrized by the angle φ of the polar coordinate system centered at $\underset{\sim}{u}_L$. Explicitly,

$$u \equiv u(\varphi) = u_L + R\cos\varphi ,$$

$$v \equiv v(\varphi) = v_L + R\sin\varphi$$

where

$$R \equiv R(\varphi) = -2\,\frac{\alpha u_L + \beta v_L}{\alpha\cos\varphi + \beta\sin\varphi} ,$$

$$\alpha \equiv \alpha(\varphi) = b_1\sin^2\varphi + (a_1 - b_2)\sin\varphi\cos\varphi - a_2\cos^2\varphi ,$$

$$\beta \equiv \beta(\varphi) = c_1\sin^2\varphi + (b_1 - c_2)\sin\varphi\cos\varphi - b_2\cos^2\varphi .$$

For system (3) with $b = 0$, these become

$$\alpha \equiv (a-1)\sin\varphi\cos\varphi ,$$

$$\beta \equiv 1 .$$

In particular

$$\lim_{\varphi \to 0^-} |u| = \infty \qquad \lim_{\varphi \to 0^-} v = \frac{a-2}{a}\, v_L$$

$$\lim_{\varphi \to -\pi^+} |u| = \infty \qquad \lim_{\varphi \to -\pi^+} v = \frac{a-2}{a}\, v_L .$$

THE AXES $H(\underset{\sim}{0})$: For system (1), the Hugoniot locus of the origin consists of the lines determined by the cubic equation

$$-a_2u^3 + (a_1 - 2b_2)u^2v + (2b_1 - c_2)uv^2 + c_1v^3 = 0 .$$

For system (3), the equation is

$$-bu^3 + (a - 2)u^2v + 2buv^2 + v^3 = 0 .$$

For $b = 0$, the equation is

$$(a - 2)u^2v + v^3 = 0 .$$

THE LINES $\lambda = 0$: For system (1), the lines $\lambda = 0$ satisfy the quadratic equation

$$(a_1b_2 - b_1a_2)u^2 + (a_1c_2 - c_1a_2)uv + (b_1c_2 - c_1b_2)v^2 = 0 .$$

For system (3), the equation is

$$(a - b^2)u^2 - buv - v^2 = 0 .$$

For $b = 0$, the equation is

$$au^2 - v^2 = 0 .$$

In particular, for $a > 0$ and $b = 0$, the set of states $\underset{\sim}{u}$ for which $\lambda(\underset{\sim}{u}) = 0$ consists of the two lines through the origin with slopes

$$\frac{v}{u} = \pm \sqrt{a} .$$

The role of the lines $\lambda = 0$ in the classification of the integral curves: [see Figure 8]. In Region I, $\lambda = 0$ if and only if $\underset{\sim}{u} = 0$. The boundary between Regions I and II is the set of systems (3) for which the line $\lambda = 0$ coincides with a line in the Hugoniot locus of the origin. Crossing into Region II, this line splits into two lines, and systems in Region II are precisely those which satisfy the condition that the lines $\lambda = 0$ cut through the interiors of the four sectors closest to the u-axis which are determined by the Hugoniot locus of the origin. The boundary between Region II and Region III consists of the systems (3) for which the lines $\lambda = 0$ coincide with two lines other than the u-axis in the Hugoniot locus of the origin. And finally, the systems in Region III are characterized by the condition that the lines $\lambda = 0$ cut through the interiors of the two middle sectors determined by the Hugoniot locus of the origin.

REFERENCES

[1] Aris, R. and Amundsen, N., Mathematical Methods in Chemical Engineering, Vol. 2, Prentice-Hall, Inc., Englewood Cliffs, New Jersey.

[2] Courant, R. and Friedrichs, K. O., Supersonic Flow and Shock Waves, Wiley, New York, 1948.

[3] Darboux, G., Theorie General des Surfaces, Chelsea, New York, 1972.

[4] Glimm, J., "Solutions in the large for nonlinear hyperbolic systems of equations", Comm. Pure Appl. Math., 18 (1965), 697-715.

[5] Helfferich, F. and Klein, G., Multicomponent Chromatography, Marcel Dekker, Inc., New York, 1970.

[6] Isaacson, E., "Global solution of a Riemann problem for a non-strictly hyperbolic system of conservation laws arising in enhanced oil recovery", J. Comp. Phys., to appear.

[7] Isaacson, E. and Temple, B., "Analysis of a singular hyperbolic system of conservation laws", J. Diff. Eqn. (to appear).

[8] Isaacson, E. and Temple, B., "Examples and classification of non-strictly hyperbolic systems of conservation laws", Abstracts of the AMS, Jan., 1985. Presented in the Special Session on "Non-Strictly Hyperbolic Conservation Laws" at the Winter Meeting of AMS, Anaheim, Jan., 1985.

[9] Keyfitz, B. and Kranzer, H., "A system of non-strictly hyperbolic conservation laws arising in elasticity theory", Arch. Rat. Mech. Anal., 72 (1980).

[10] Keyfitz, B. L. and Kranzer, H. C., "The Riemann problem for a class of conservation laws exhibiting a parabolic degeneracy", J. Diff. Eqn., 47 (1983), 35-65.

[11] Lax, P. D., "Hyperbolic systems of conservation laws, II", Comm. Pure Appl. Math., 19 (1957), 537-566.

[12] Lax, P. D., "Shock waves and entropy", in Contributions to Nonlinear Functional Analysis, ed. E. H. Zarantonello, Academic Press, New York, 1971, 603-634.

[13] LeVeque, Randall J. and Temple, Blake, "Stability of Godunov's method for a class of 2 × 2 systems of conservation laws", Trans. Amer. Math. Soc., 288, No. 1, (1985).

[14] Liu, T. P., "The Riemann problem for general 2 × 2 conservation laws", Trans. Amer. Math. Soc., 199 (1974), 89-112.

[15] Marchesin, D. and Paes-Leme, P. J., unpublished manuscript.

[16] Rhee, H., Aris, R. and Amundsen, N. R., "On the theory of multicomponent chromatography", Phil. Trans. Roy. Soc., A267, 419 (1970).

[17] Schaeffer, D. G. and Shearer, M., "The classification of 2 × 2 systems of non-strictly hyperbolic conservation laws, with application to oil recovery", with Appendix by D. Marchesin, P. J. Paes-Leme, D. G. Schaeffer, and M. Shearer, preprint, Duke University.

[18] Shearer, M., Schaeffer, D. G., Marchesin, D. and Paes-Leme, P., "Solution of the Riemann problem for a prototype 2 × 2 system of non-strictly hyperbolic conservation laws", preprint, Duke University.

[19] Serre, Dennis, "Bounded variation solutions for some hyperbolic systems of conservation laws", J. Diff. Eqn. (to appear).

[20] Smoller, J. A., Shock waves and reaction diffusion equations, Springer-Verlag (1980).

[21] Temple, B., "Global solution of the Cauchy problem for a class of 2 × 2 non-strictly hyperbolic conservation laws", Adv. Appl. Math., 3 (1982), 335-375.

[22] Temple, B., "Systems of conservation laws with coinciding shock and rarefaction curves", Contemporary Mathematics, 17 (1983).

[23] Temple, B., "Systems of conservation laws with invariant submanifolds", Trans. Amer. Math. Soc., 280 (1983).

[24] Shearer, M., Private communication.

[25] Schaeffer, D. G., Private communication.

EI:DM:BP:BT:scr

LEGEND


1-rarefaction

1-expansive shock

1-shock

2-rarefaction

2-expansive shock

2-shock (with or without arrows)

1-composite (rarefaction followed by shock at characteristic speed)

compressive shock

crossing shock

expansive shock

2-boundary, triple shock curves

Hugoniot locus of $\underset{\sim}{u}_L$ and u-axis

NOTE 1: Arrows on rarefaction curves indicate the direction of increasing eigenvalue. Arrows on shock curves indicate the direction of decreasing shock speed.

NOTE 2: 1- and 2-shocks in the Hugoniot locus of $\underset{\sim}{u}_L$ are indicated by dashed lines supported by the solid line for the Hugoniot locus.

Figure Captions

Figure 1: Integral curves for the symmetric systems in Region IV; i.e., system (3) with $b = 0$, $a > 2$. (*Family 1 is denoted by the thicker lines.*)

Figure 2: The Sectors A_1, A_2 determined by the ray $\theta = \theta_*$ ($\lambda_1 = 0$).

Figures 3A-F: Hugoniot loci and shock types for $\underset{\sim}{u}_L$ in representative positions.

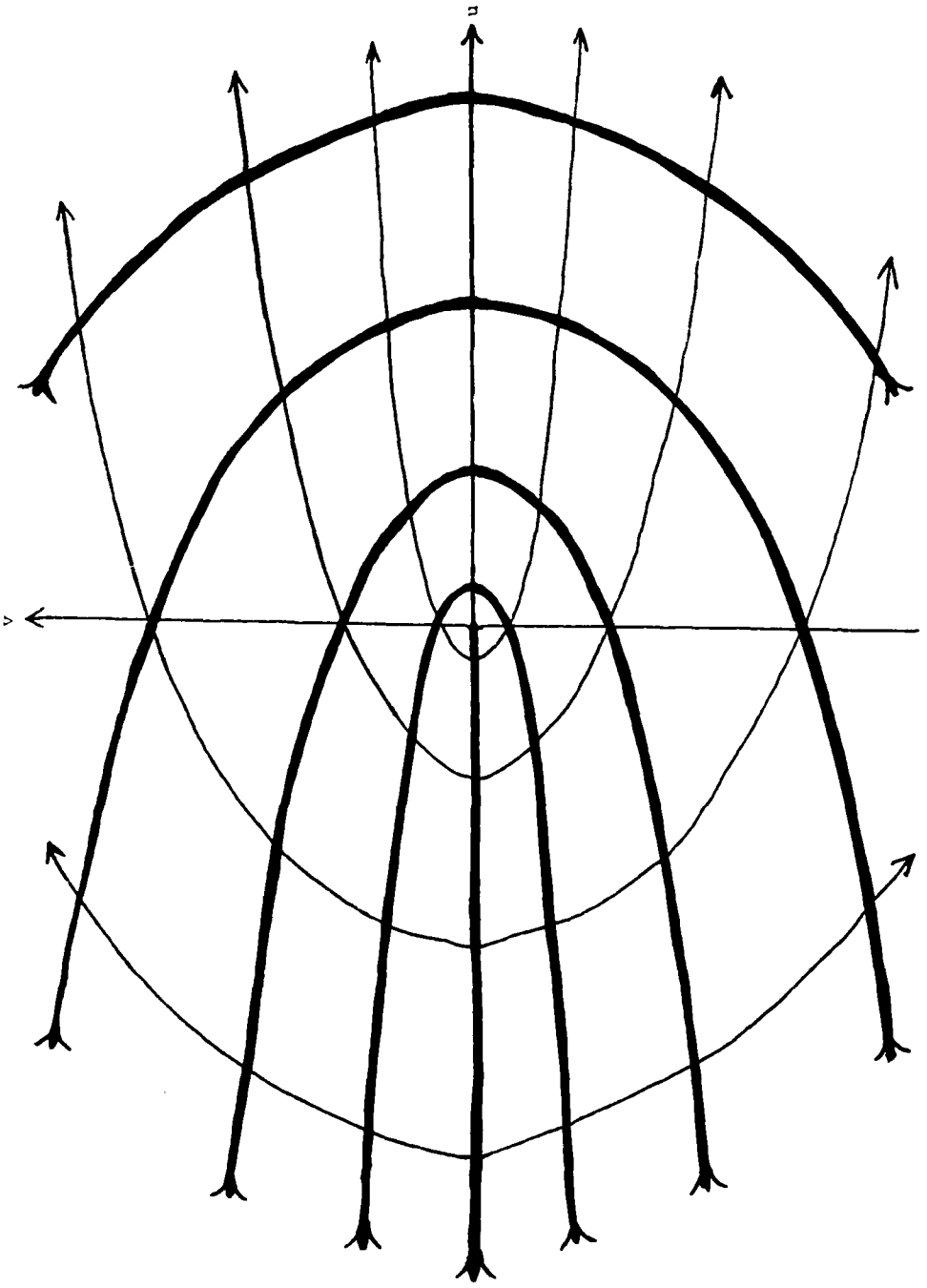

Figure 1

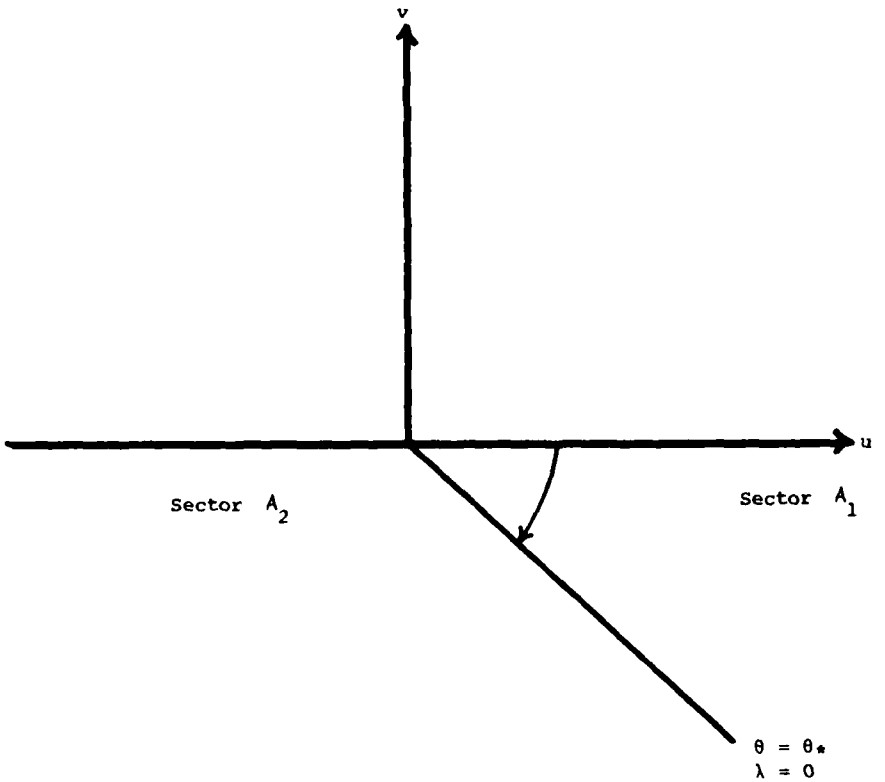

Figure 2

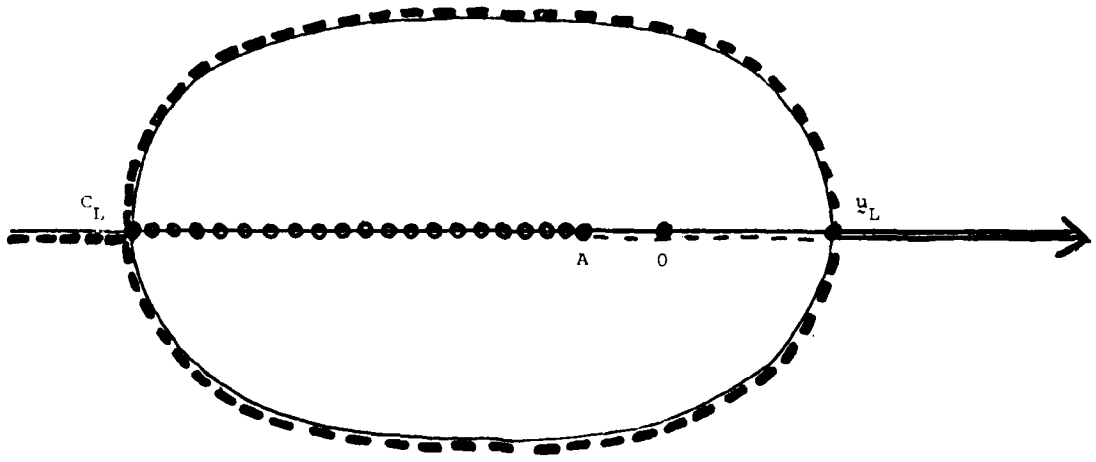

Figure 3A

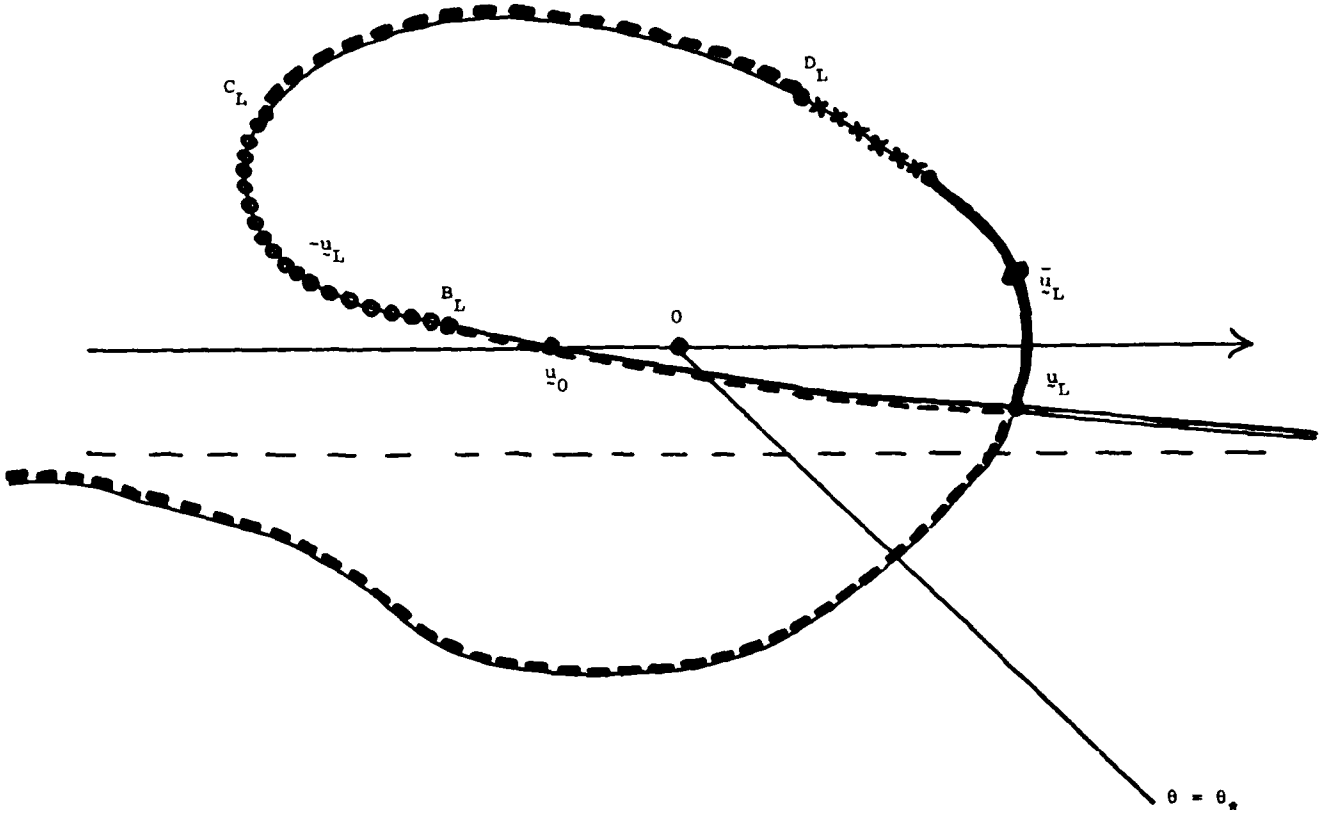
C_L
D_L
$-\underset{\sim}{u}_L$
B_L
0
$\underset{\sim}{u}_0$
$\bar{\underset{\sim}{u}}_L$
$\underset{\sim}{u}_L$
$\theta = \theta_*$

Figure 3B

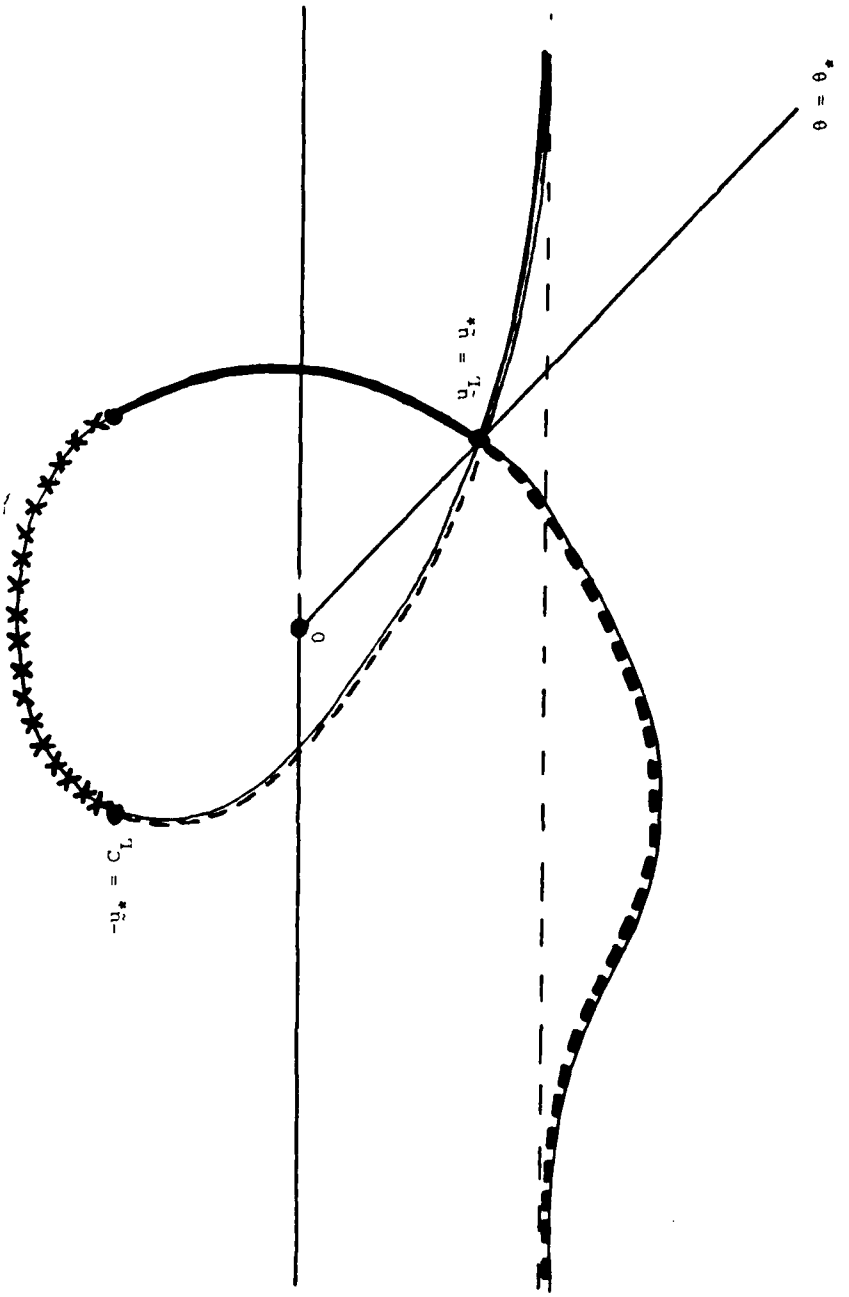

Figure 3C

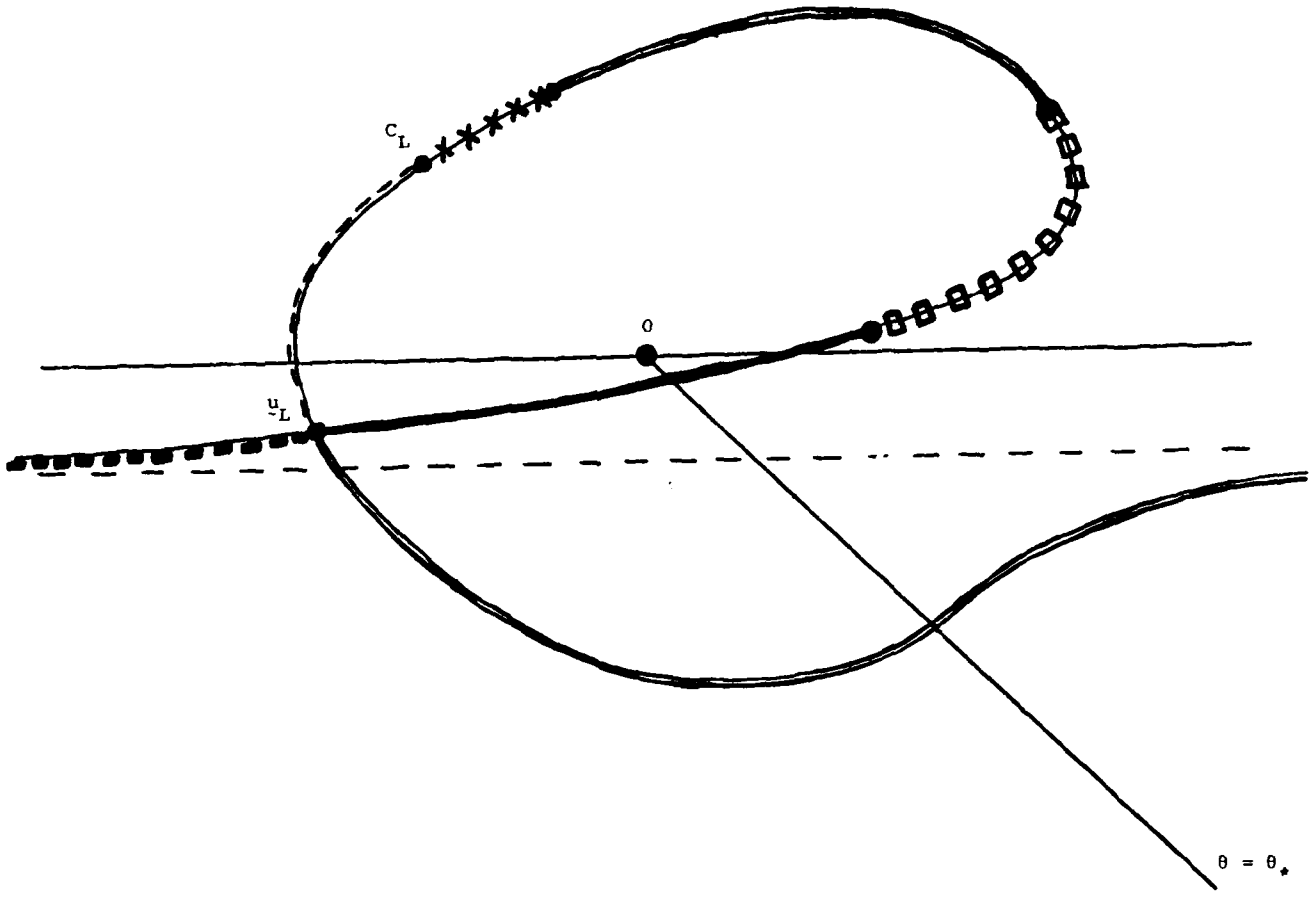

Figure 3D

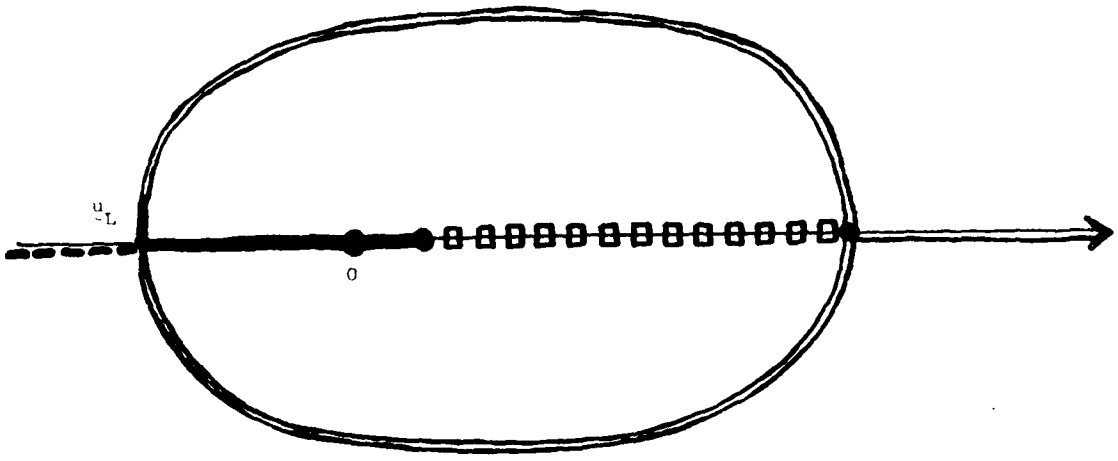

Figure 3E

$\underset{\sim}{u}_L = \underset{\sim}{0}$

Figure 3F

Figure 4A: 1RS-composite wave in x,t-space.

Figure 4B: 2SR-composite wave in x,t-space.

Figure 5: Typical curves:

Rarefaction ($R_1(\underset{\sim}{u})$ = [$\underset{\sim}{u}$FE]),

1-Composite ($C_1(F)$ = [ED]),

2-Boundary ([∞CC_*]),

Triple Shock ([ABC_*]).

Figure 6A: The wave curves for $\underset{\sim}{u}_L \in A_1$.

Figure 6B: The wave curves for $\underset{\sim}{u}_L \in A_2$.

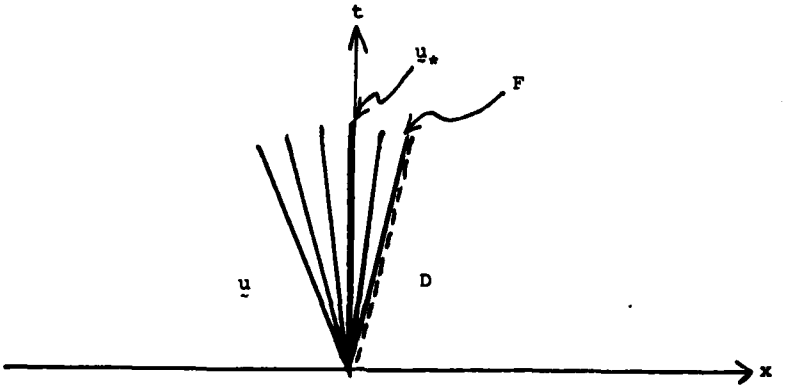

1RS-COMPOSITE WAVE

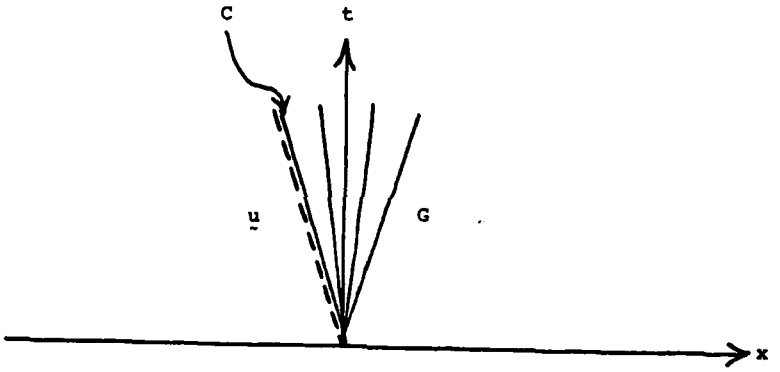

2SR-COMPOSITE WAVE

Figures 4A, 4B

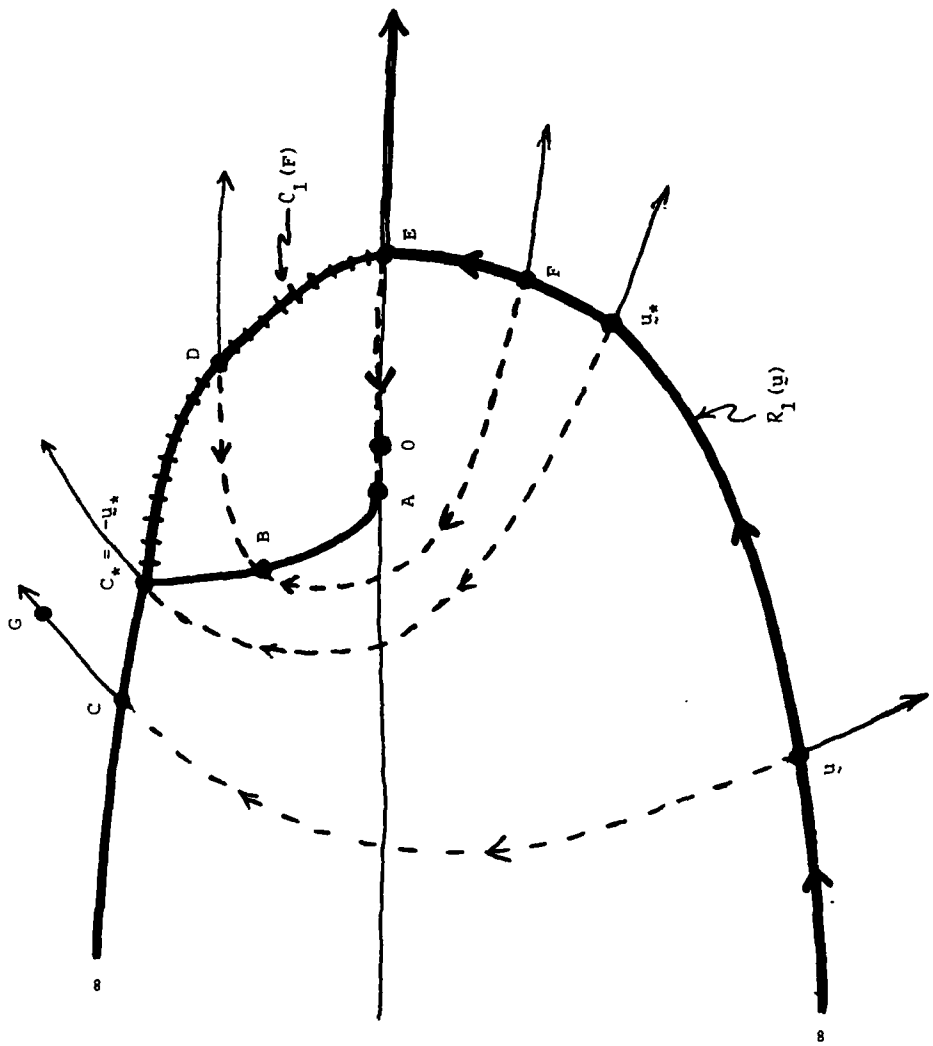

Figure 5

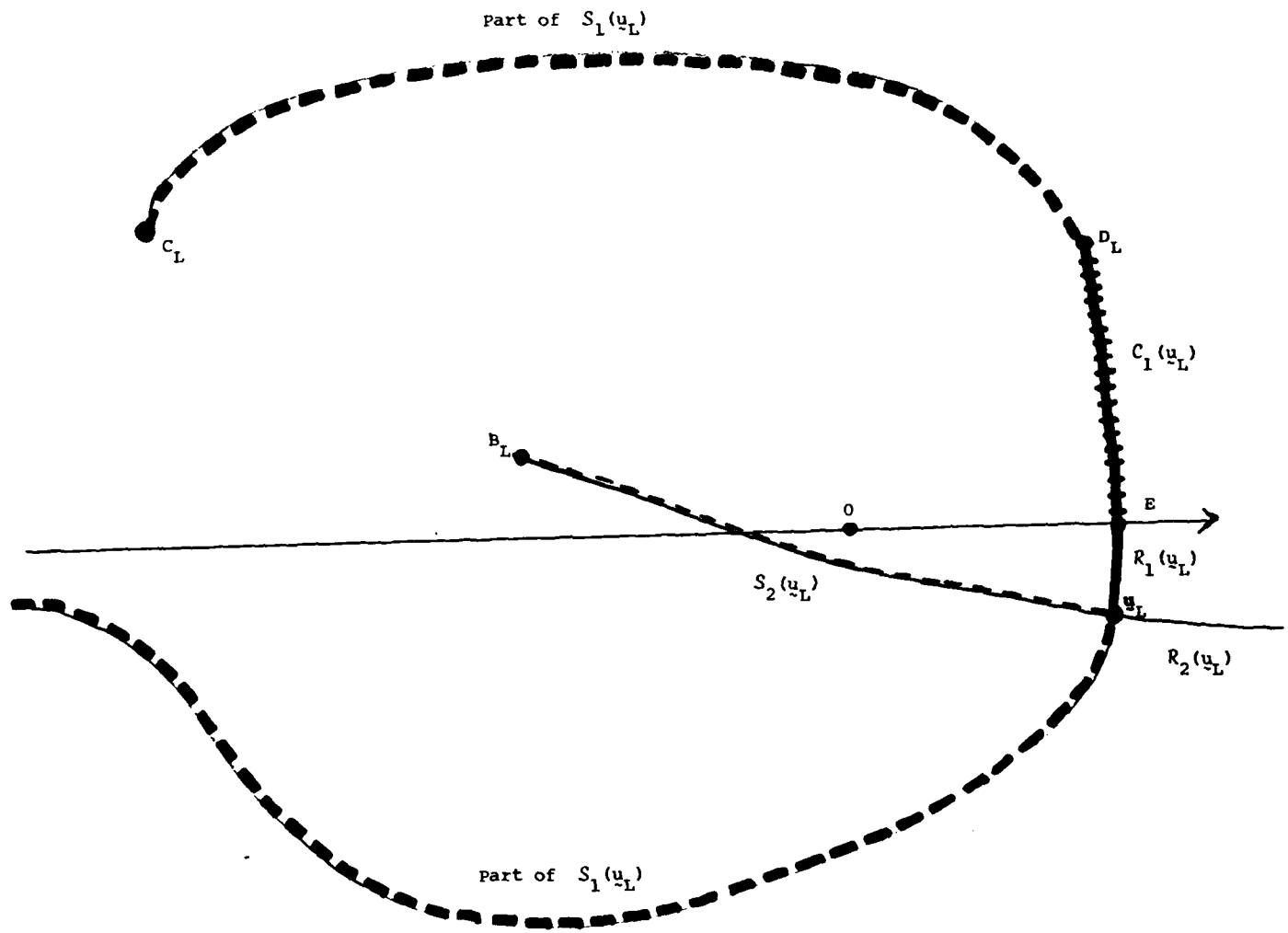

Figure 6A: The Wave Curves for $u_L \in A_1$

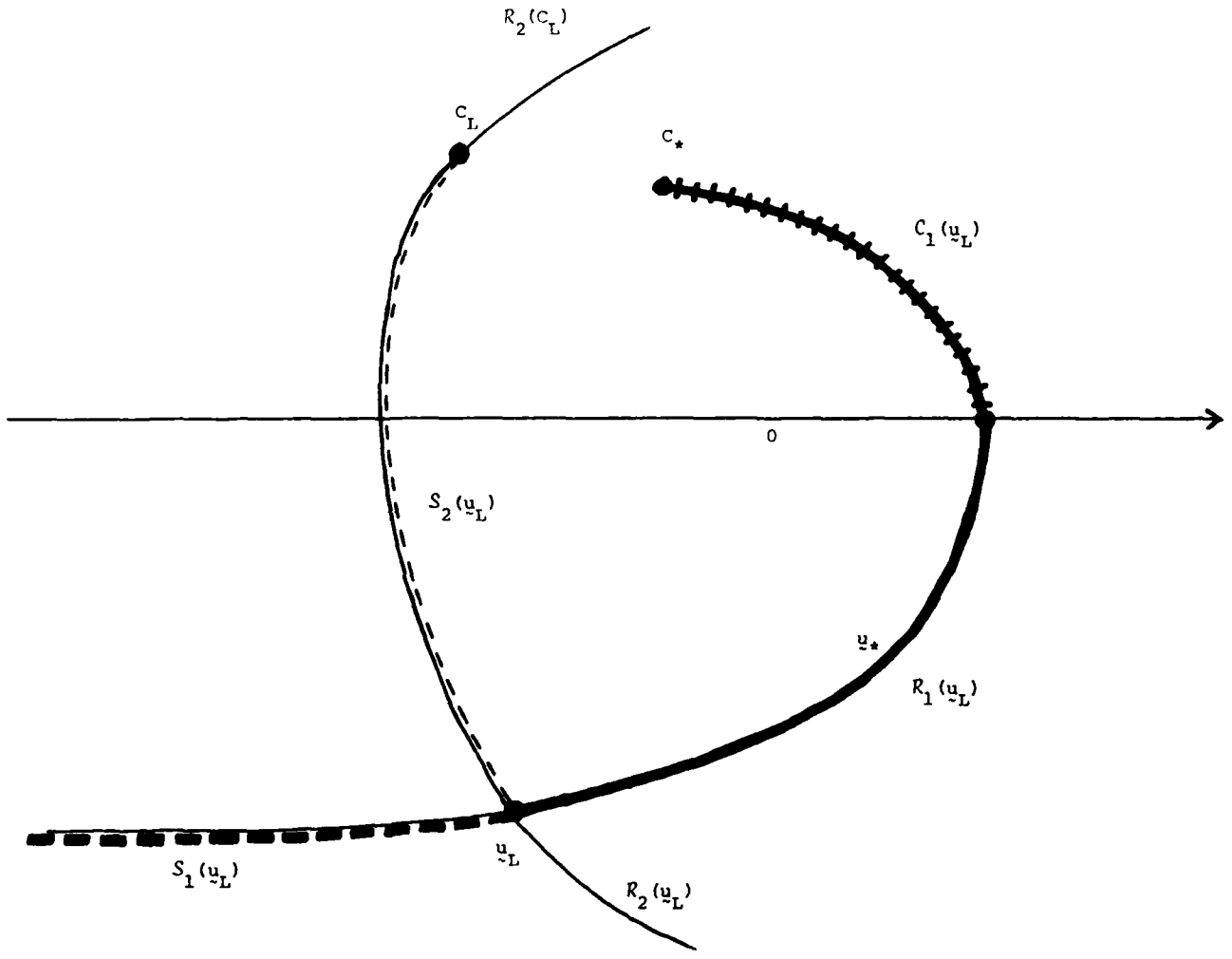

Figure 6B: The Wave Curves for $u_L \in A_2$

Figure 7A: Riemann problem solution for $\theta_L = 0$.

Figure 7B: Riemann problem solution for $\underset{\sim}{u}_L \in A_1$.

Figure 7C: Riemann problem solution for $\theta_L = \theta_*$.

Figure 7D: Riemann problem solution for $\underset{\sim}{u}_L \in A_2$.

Figure 7E: Riemann problem solution for $\theta_L = -\pi$.

Figure 7F: Riemann problem solution for $\underset{\sim}{u}_L = \underset{\sim}{0}$.

Figures 8A-D: Relationship between the axes and the lines $\lambda = 0$ for Regions I-IV.

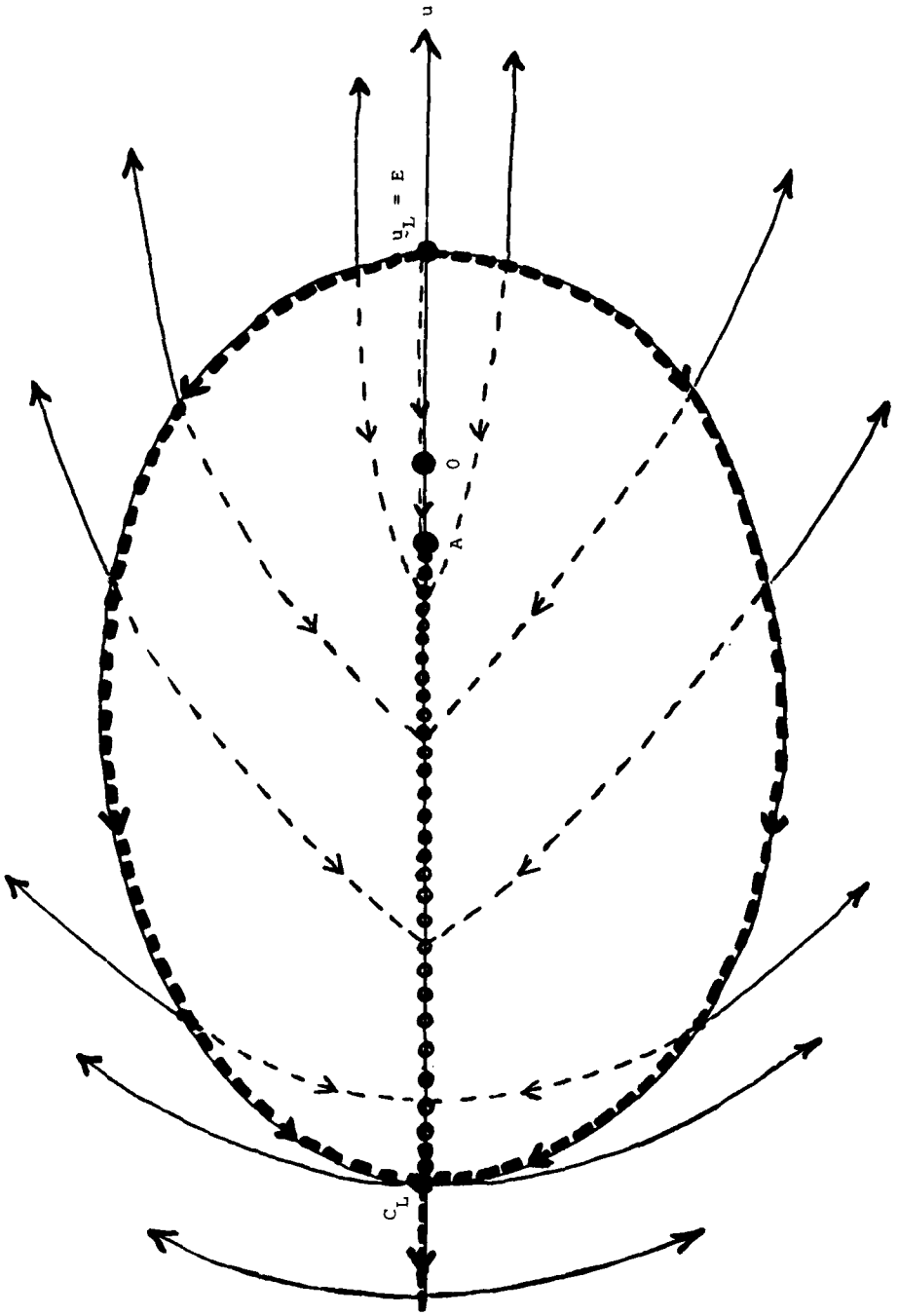

Figure 7A

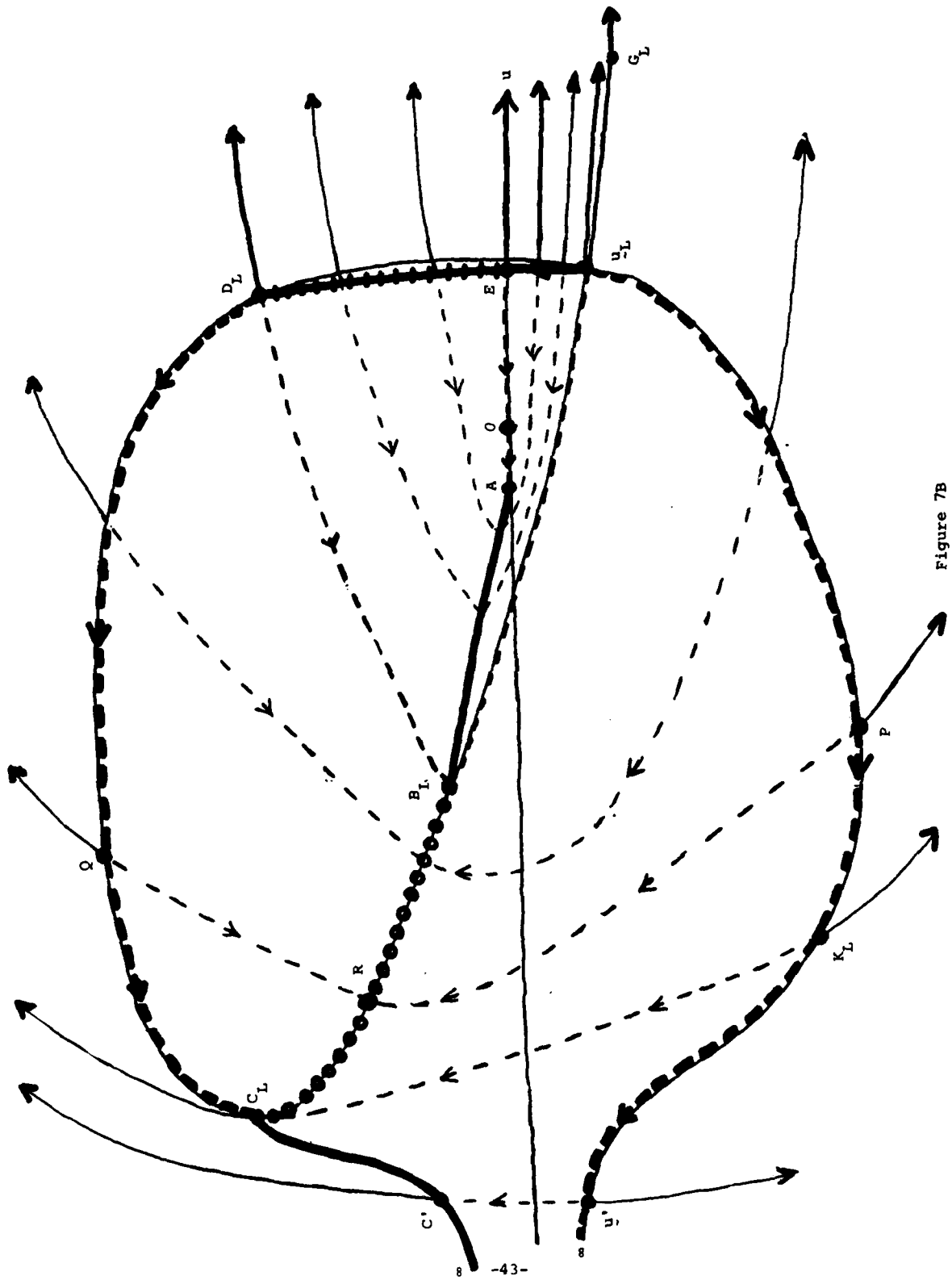

Figure 7B

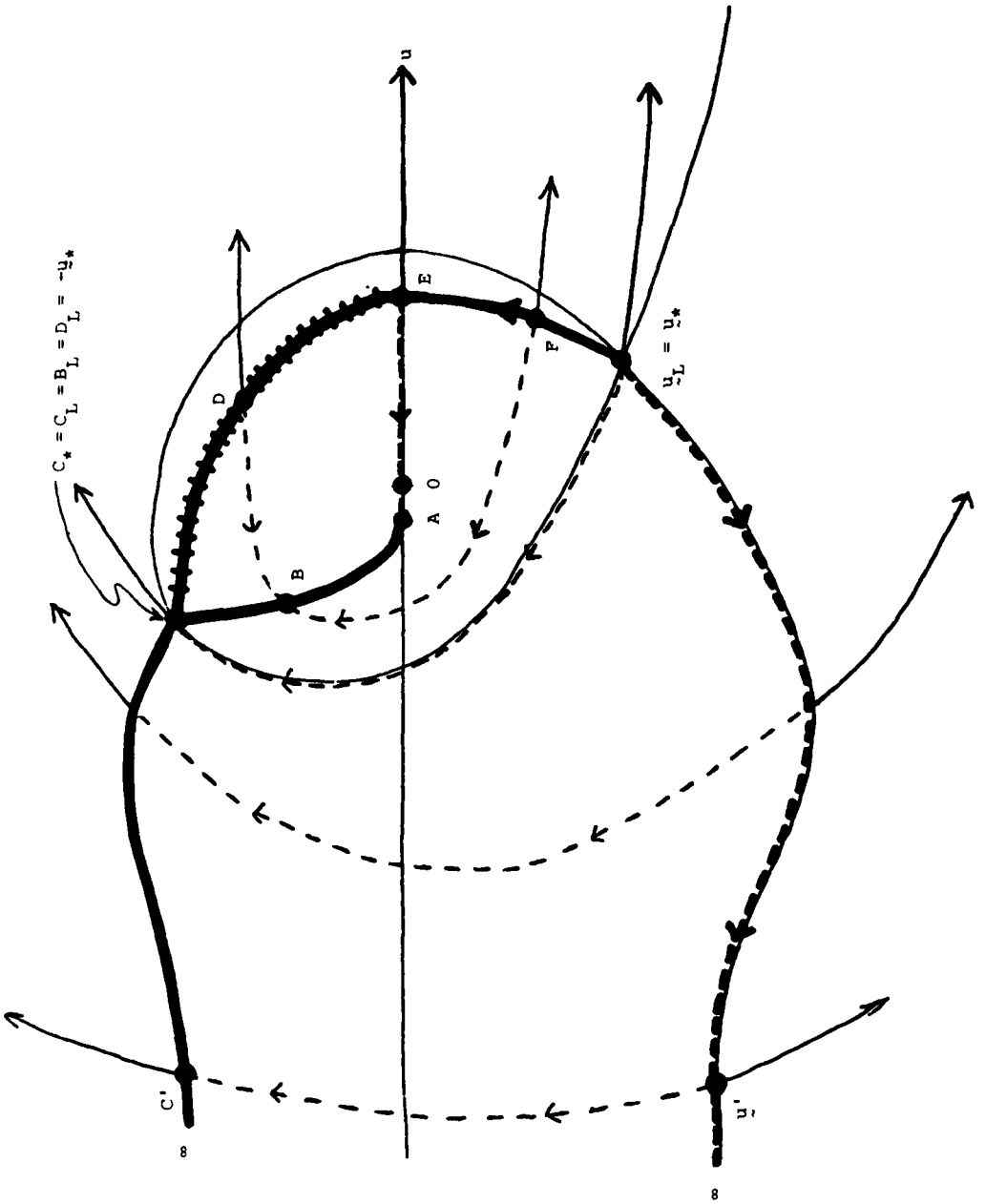

Figure 7C

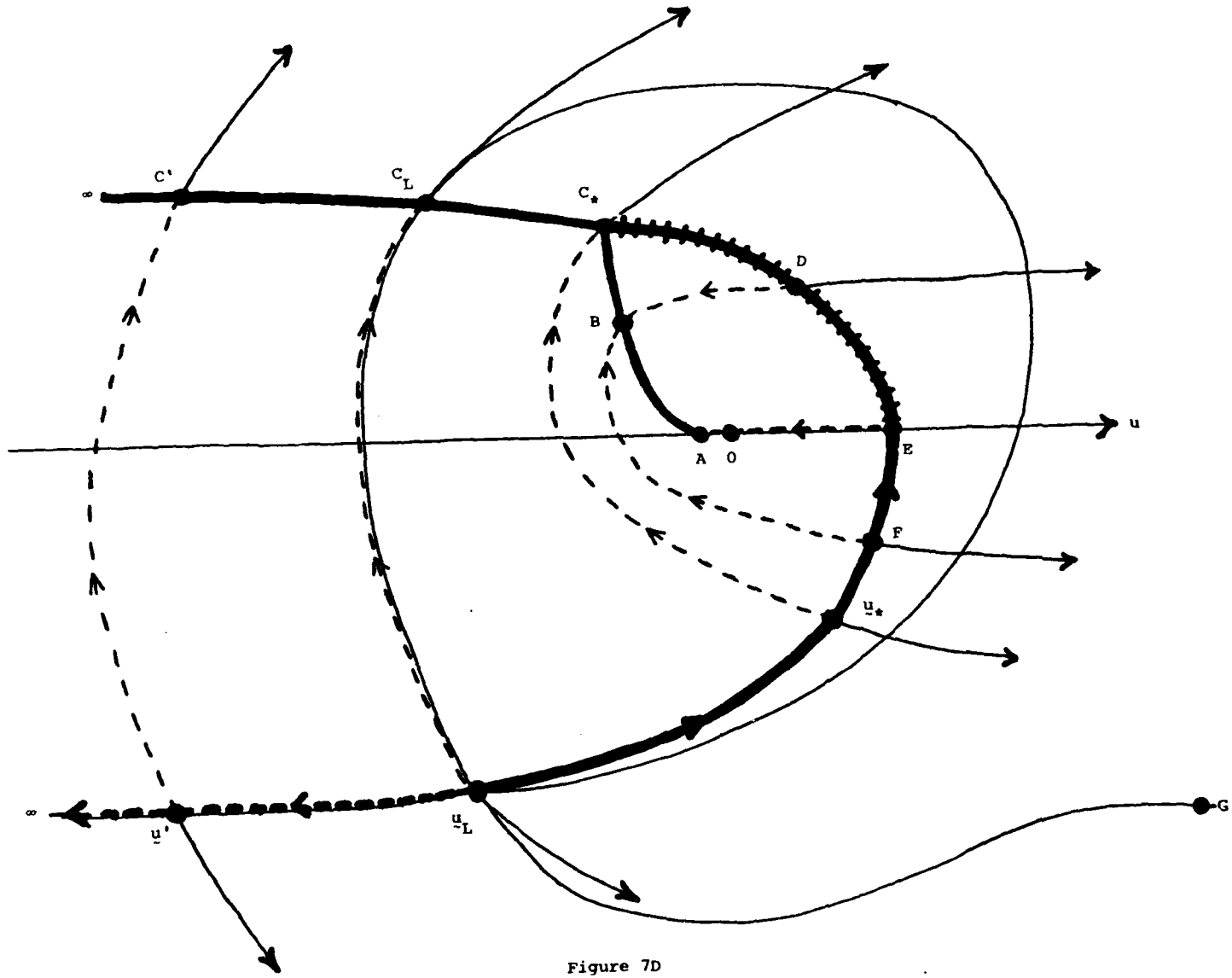

Figure 7D

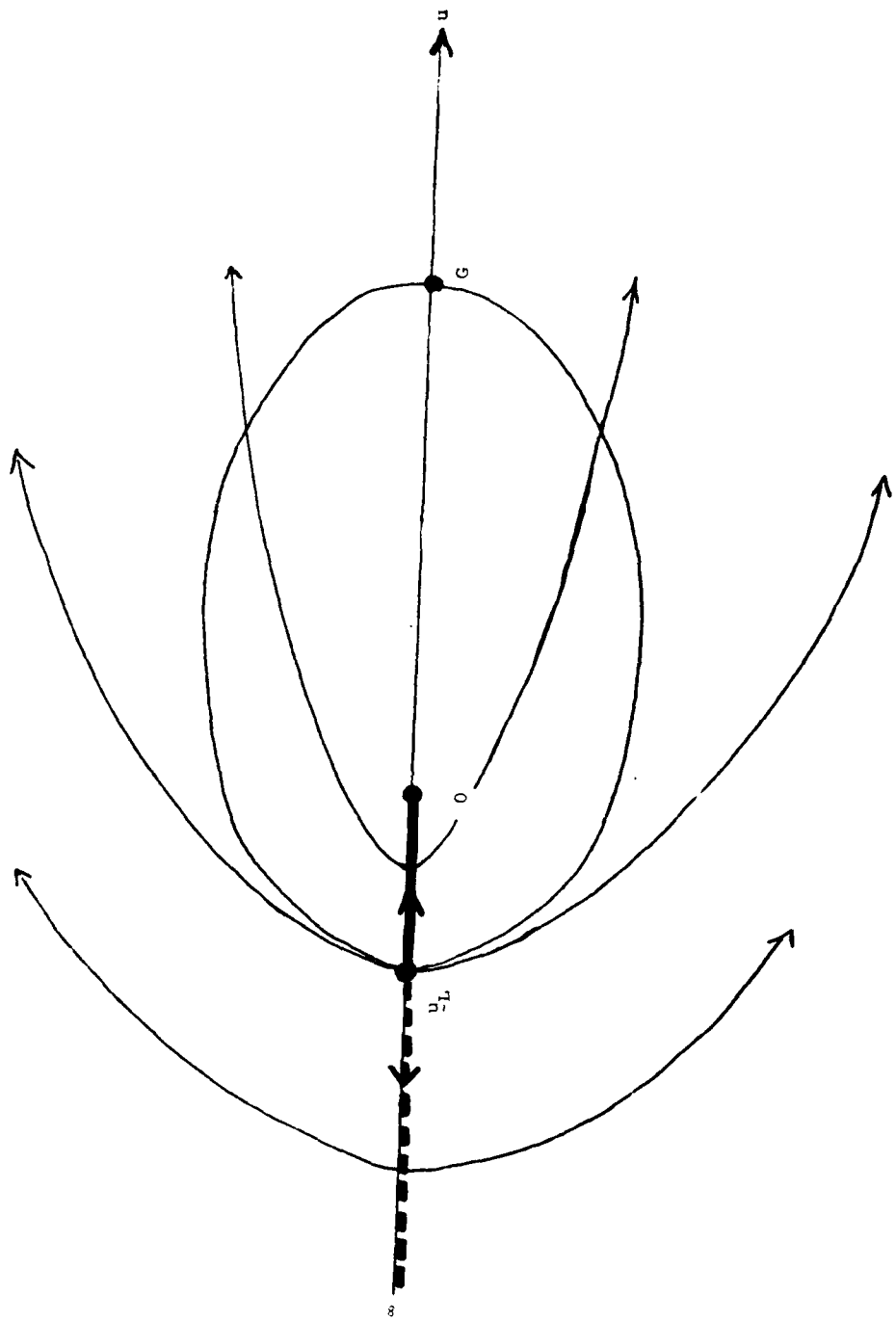

Figure 7E

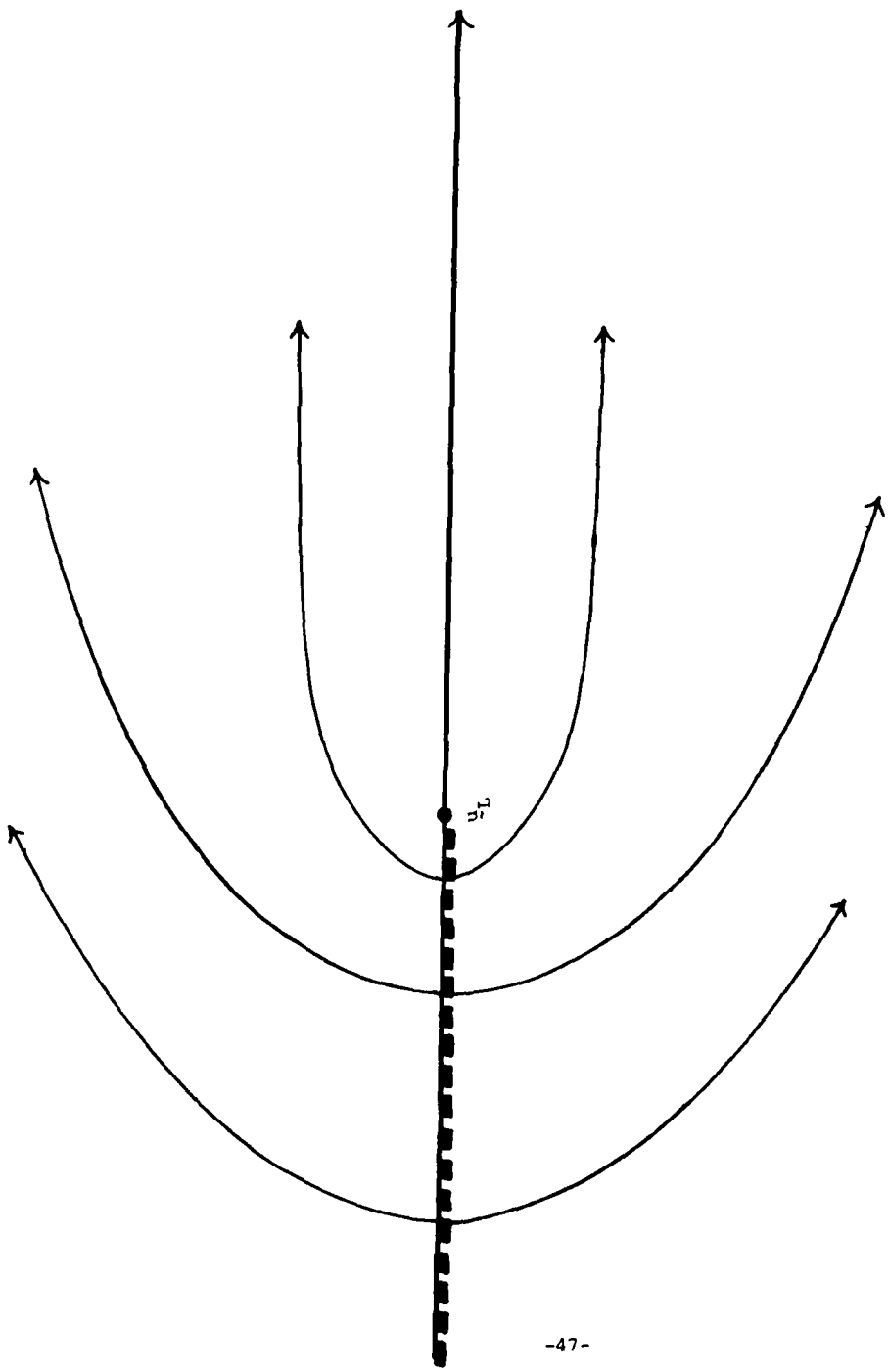

Figure 7F

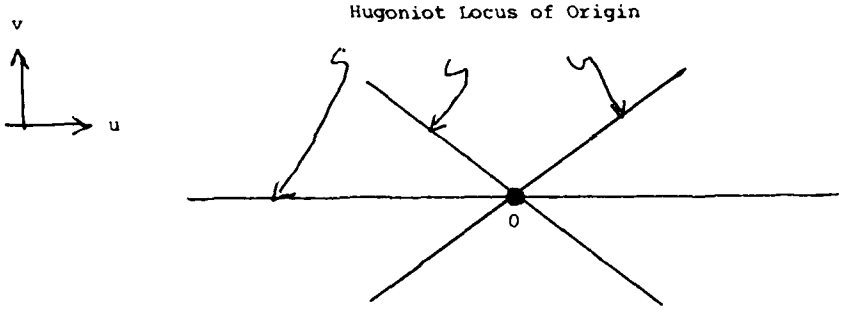

Region I: $\lambda = 0$ if and only if $\underset{\sim}{u} = 0$.

Figure 8A

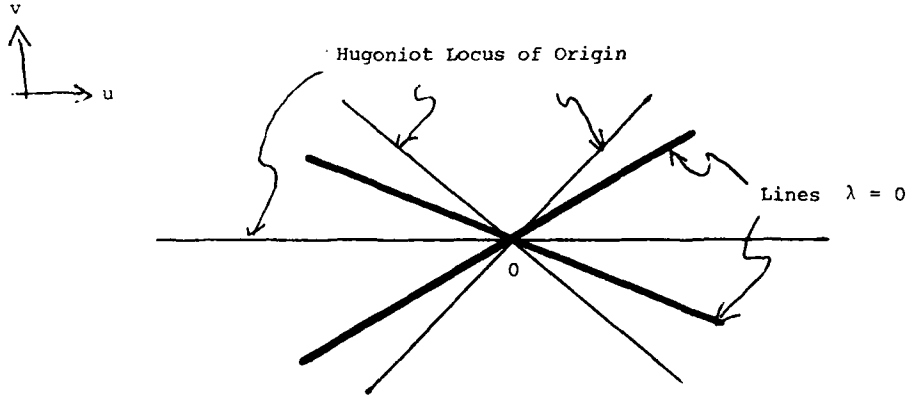

Region II

Figure 8B

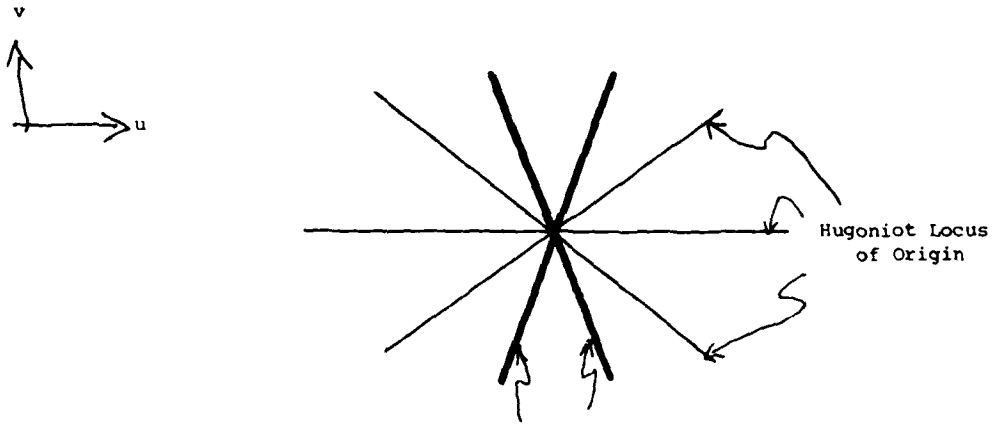

Region III

Figure 8C

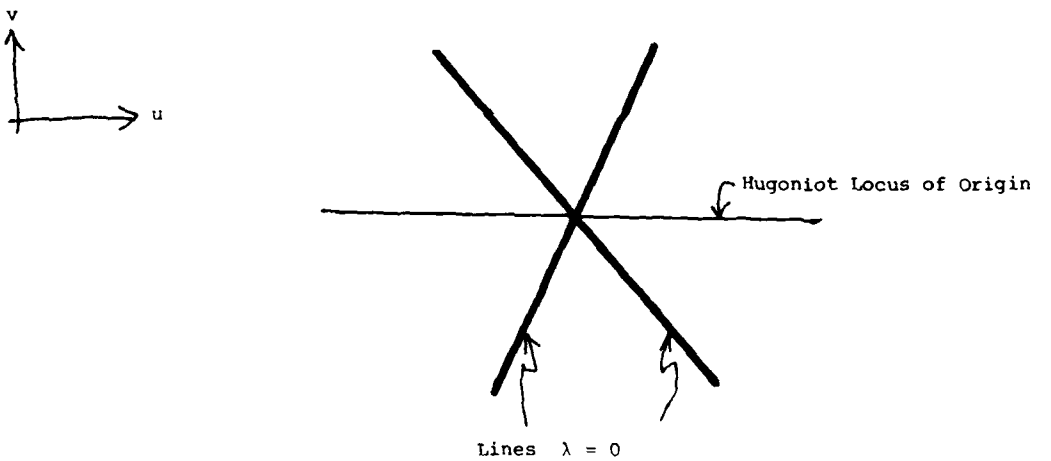

Region IV

Figure 8D

SECURITY CLASSIFICATION OF THIS PAGE *(When Data Entered)*

REPORT DOCUMENTATION PAGE		READ INSTRUCTIONS BEFORE COMPLETING FORM
1. REPORT NUMBER 2891	2. GOVT ACCESSION NO. AD-A163706	3. RECIPIENT'S CATALOG NUMBER
4. TITLE *(and Subtitle)* THE CLASSIFICATION OF SOLUTIONS OF QUADRATIC RIEMANN PROBLEMS (I)		5. TYPE OF REPORT & PERIOD COVERED Summary Report - no specific reporting period 6. PERFORMING ORG. REPORT NUMBER
7. AUTHOR(s) E. Isaacson, D. Marchesin, B. Plohr and B. Temple		8. CONTRACT OR GRANT NUMBER(s) DAAG29-80-C-0041 DMS-8210950, Mod. 1
9. PERFORMING ORGANIZATION NAME AND ADDRESS Mathematics Research Center, University of Wisconsin 610 Walnut Street Madison, Wisconsin 53705		10. PROGRAM ELEMENT, PROJECT, TASK AREA & WORK UNIT NUMBERS Work Unit Numbers 1 - Applied Analysis & 3 - Numerical Analysis & Scientific Computing
11. CONTROLLING OFFICE NAME AND ADDRESS See Item 18 below.		12. REPORT DATE December 1985 13. NUMBER OF PAGES 49
14. MONITORING AGENCY NAME & ADDRESS*(if different from Controlling Office)*		15. SECURITY CLASS. *(of this report)* UNCLASSIFIED 15a. DECLASSIFICATION/DOWNGRADING SCHEDULE

16. DISTRIBUTION STATEMENT *(of this Report)*

Approved for public release; distribution unlimited.

17. DISTRIBUTION STATEMENT *(of the abstract entered in Block 20, if different from Report)*

18. SUPPLEMENTARY NOTES

U. S. Army Research Office
P. O. Box 12211
Research Triangle Park
North Carolina 27709

National Science Foundation
Washington, D. C. 20550

19. KEY WORDS *(Continue on reverse side if necessary and identify by block number)*

Riemann problem
non-strictly hyperbolic conservation laws
umbilic points

20. ABSTRACT *(Continue on reverse side if necessary and identify by block number)*

We are interested in classifying the solutions of Riemann problems for the 2×2 conservation laws which have homogeneous quadratic flux functions. Such flux functions approximate an arbitrary 2×2 system in a neighborhood of an isolated point where strict hyperbolicity fails. This problem was motivated by Marchesin and Paes-Leme who discovered such a singularity in a system of equations arising in oil reservoir simulation [15,17]. In [18], Schaeffer, Shearer, Marchesin and Paes-Leme solved the Riemann problem for this system in a neighborhood of the singular point. In [8], Isaacson and Temple outlined a

DD FORM 1 JAN 73 1473 EDITION OF 1 NOV 65 IS OBSOLETE

UNCLASSIFIED

SECURITY CLASSIFICATION OF THIS PAGE *(When Data Entered)*

20. ABSTRACT - cont'd.

program for classifying such singularities by means of locating normal forms for the equivalence classes of equations generated by linear changes in dependent variables. A 2-parameter family of such normal forms was found by Plohr. In the important work of Schaeffer and Shearer [17], a new normal form was found which reduced the classification of integral curves to a theorem of Darboux on the classification of umbilic points for homogeneous cubic equations [3]. The integral curves fall into four isomorphism classes, called Regions I-IV. In this paper we give the solution of the Riemann problem for the systems in Region IV which exhibit up-down symmetry. A presentation of the solutions of the corresponding systems in Regions II and III will follow.

Our analysis uses a numerical determination of the Hugoniot loci. Moreover, a new phenomenon occurs in Regions II-IV that does not occur in Region I: lines exist on which one of the eigenvalues has the value of the eigenvalue at the singular point. Bifurcations occur at these lines, and the dynamics of the lines as the parameters in the normal form are varied gives a geometric interpretation of the boundaries between Regions I-III. The program for classifying hyperbolic singular points in 2×2 systems of conservation laws is being carried out jointly by the authors named above.

END

FILMED

3-86

DTIC